HHS Public Access

Author manuscript

Cell Rep. Author manuscript; available in PMC 2023 February 28.

Published in final edited form as:

Cell Rep. 2023 January 31; 42(1): 112005. doi:10.1016/j.celrep.2023.112005.

CDK1 bridges NF-κB and β-catenin signaling in response to *H. pylori* infection in gastric tumorigenesis

Shoumin Zhu[1,6], **Marwah Al-Mathkour**[1,6], **Longlong Cao**[1,2,6], **Shayan Khalafi**[1], **Zheng Chen**[1,4], **Julio Poveda**[3], **Dunfa Peng**[1], **Heng Lu**[1], **Mohammed Soutto**[1], **Tianling Hu**[1], **Oliver G. McDonald**[3], **Alexander Zaika**[1,4,5], **Wael El-Rifai**[1,4,5,7,*]

[1]Department of Surgery, Miller School of Medicine, University of Miami, Miami, FL, USA

[2]Department of Gastric Surgery, Fujian Medical University Union Hospital, Fuzhou, China

[3]Department of Pathology, Miller School of Medicine, University of Miami, Miami, FL, USA

[4]Sylvester Comprehensive Cancer Center, Miller School of Medicine, University of Miami, Miami, FL, USA

[5]Department of Veterans Affairs, Miami Healthcare System, Miami, FL, USA

[6]These authors contributed equally

[7]Lead contact

SUMMARY

Infection with *Helicobacter pylori* (*H. pylori*) is the main risk factor for gastric cancer, a leading cause of cancer-related death worldwide. The oncogenic functions of cyclin-dependent kinase 1 (CDK1) are not fully understood in gastric tumorigenesis. Using public datasets, quantitative real-time PCR, western blot, and immunohistochemical (IHC) analyses, we detect high levels of CDK1 in human and mouse gastric tumors. *H. pylori* infection induces activation of nuclear factor κB (NF-κB) with a significant increase in CDK1 in *in vitro* and *in vivo* models ($p < 0.01$). We confirm active NF-κB binding sites on the CDK1 promoter sequence. CDK1 phosphorylates and inhibits GSK-3β activity through direct binding with subsequent accumulation and activation of β-catenin. CDK1 silencing or pharmacologic inhibition reverses these effects and impairs tumor organoids and spheroid formation. IHC analysis demonstrates a positive correlation between CDK1 and β-catenin. The results demonstrate a mechanistic link between infection, inflammation, and gastric tumorigenesis where CDK1 plays a critical role.

*Correspondence: wxe45@miami.edu.

AUTHOR CONTRIBUTIONS

Conceptualization, S.Z. and W.E-R.; development of methodology, S.Z., M.A-M., H.L., L.C., and M.S.; analysis and interpretation of data, S.Z., M.A-M., H.L., Z.C., D.P., and W.E-R.; writing and revision of the manuscript, S.Z., M.A-M., and W.E-R.; administrative, technical, or material support, O.G.M., A.Z., T.H., S.K., and J.P.; study supervision, W.E-R.

SUPPLEMENTAL INFORMATION

Supplemental information can be found online at https://doi.org/10.1016/j.celrep.2023.112005.

DECLARATION OF INTERESTS

The authors declare no conflict of interest.

In brief

Zhu et al. show induction of CDK1 in response to *H. pylori* infection via NF-κB-dependent transcription regulation. CDK1-mediated activation of β-catenin signaling, promoting expansion of cancer cells. The results demonstrate a mechanistic link between infection, inflammation, and gastric tumorigenesis where CDK1 plays a critical role.

Graphical Abstract

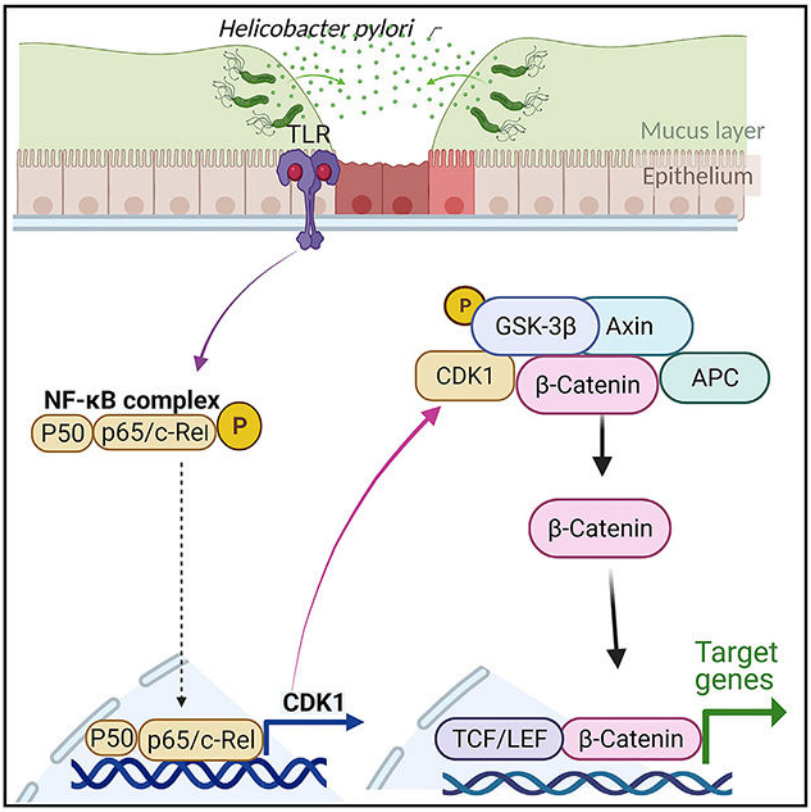

INTRODUCTION

Gastric cancer is a leading cause of cancer-related death worldwide.[1] Most patients with gastric cancer in the United States are diagnosed at a late stage (stages III and IV), with a poor 5-year survival rate.[2] Therefore, identifying signaling pathways and druggable molecular vulnerabilities relevant to the biology of gastric cancer are important approaches to improve our diagnostic, preventive, and therapeutic strategies in the fight against gastric cancer.

Helicobacter pylori (*H. pylori*) is a spiral-shaped gram-negative bacteria that colonizes the human stomach. *H. pylori* infection has a very high prevalence,[3] with an estimated presence in more than half of the world's population.[4] The World Health Organization has classified infection with *H. pylori* as a group 1 carcinogen.[5] *H. pylori* infection is typically acquired during childhood and persists as a chronic infection for several decades.[6] Chronic

H. pylori infection is the most established etiological factor in the development of human gastric adenocarcinoma.[6,7] We and others have shown that infection with *H. pylori* promotes gastric tumorigenesis.[8–10] Infection initiates a chronic inflammatory environment with histopathologic progression from chronic gastritis to gastric atrophy, intestinal metaplasia, dysplasia, and finally, gastric cancer.[7,11] *H. pylori* infection can also activate several oncogenic signaling pathways such as WNT/β-catenin, EGFR, and FAK.[6,12]

Inflammation plays an important role in the development and progression of several cancers.[13] Nuclear factor κB (NF-κB) comprises a family of inducible transcription factors that regulate many genes involved in response to both injury and infection.[14] NF-κB is one of the most important molecules linking chronic inflammation to cancer. NF-κB activation occurs in cancer cells as well as the tumor microenvironment of most solid cancers and hematopoietic malignancies.[13] When cells are exposed to the appropriate activating stimuli, such as tumor necrosis factor (TNF), this causes the inhibitor of κB kinase to facilitate the phosphorylation-dependent ubiquitination and destruction of the inhibitor of κB (IκB) proteins (IKK).The free NF-κB translocates to the nucleus and induces transcription of a wide-range of target genes that regulate key biological cellular processes.[15] In addition to its role in the survival of cancer cells, NF-κB activation has been described in cancer stem cells, where it can promote a pro-inflammatory environment, inhibit apoptosis, and stimulate cellular expansion.[16]

Cyclin-dependent kinases (CDKs) are serine/threonine kinases that control cell-cycle progression and other critical functions.[17] Cell division is closely linked to DNA damage response (DDR) maintaining genetic integrity and cellular homeostasis.[18] CDK1 belongs to the family of CDKs that play a central role in cell-cycle progression, which drives cells through the G2 phase to mitosis.[17] There are increasing lines of evidence supporting the role of CDK1 in the DDR, particularly in DNA repair by homologous recombination and activation of the checkpoint response. Of note, overexpression and accumulation of cytoplasmic CDK1 are associated with cancer growth and poor survival rate in ovarian cancer.[19]

The Wnt/β-catenin pathway is essential for embryonic development and adult tissue homeostasis.[20] Wnt proteins block the phosphorylation and degradation of β-catenin by binding to the low-density lipoprotein receptor-related protein 5/6 and their co-receptor Frizzled.[21] Aberrant activation of the Wnt/β-catenin signaling pathway strongly correlates with tumorigenesis and progression.[22] The activation of the Wnt/β-catenin pathway is associated with gastric carcinogenesis and clinical aggressiveness.[23] The nuclear translocation and accumulation of β-catenin is necessary for transcription activation of the β-catenin/T cell factor (TCF) complex.

Although mutations in APC or CTNNB1 are a major cause of β-catenin nuclear accumulation in colorectal cancer,[24] these mutations generally occur in low frequencies (7% and 4%, respectively).[25] However, APC mutations are relatively more prevalent in the MSS/TP53+ subtype of gastric cancer than other molecular subtypes.[26]

Mechanisms of mutation-independent activation of the β-catenin pathway including upregulation of c-Met and EGFR or inhibition of tumor suppressors RUNX3 or TFF1 were observed.[23,27] Other mechanisms include upregulation of WNT receptors and ligands (FZDs and WNTs) or hypermethylation of repressors of ligand/receptors (DKK, SFRP, and RNF43).[28]

This study aimed to investigate mechanisms of upstream activation of CDK1 and its downstream functional impact on gastric tumorigenesis in response to *H. pylori* infection. Our results establish CDK1 as a transcriptional target of NF-κB induced by *H. pylori* infection. This aberrant overexpression of CDK1 mediated β-catenin accumulation and activation to promote cellular expansion and counteract infection-induced cell death in gastric carcinogenesis.

RESULTS

H. pylori infection increases CDK1 expression

To identify key genes that are abnormally expressed in gastric cancer and exclusively associated with *H. pylori* infection, we analyzed the TCGA gastric cancer cohort (including 375 tumor tissues and 32 non-tumor tissues) and local cohort 1 (whole-transcriptome sequencing data from 36 human gastric tumor tissues and matched non-tumor tissues).[29] In addition, we performed whole-transcriptome sequencing on *H. pylori* infection (PMSS1, n = 7) and uninfected C57BL/6 mouse gastric tissues (n = 7) and also on a public dataset of a C57BL/6 mouse model with *H. pylori* infection (GEO: GSE13873). We used the significance levels (|log (fold change)|>0.5 and $p < 0.05$) to identify 1,602 and 251 significant differentially expressed genes (DEGs) from the human cohort and mouse cohort, respectively. By intersecting the DEGs from the human and mouse cohorts, we finally obtained 60 DEGs containing 25 genes (including CDK1) significantly upregulated in gastric cancer (Figure 1A; Table S1). These upregulated DEGs were considered candidate genes that play an important role in gastric tumorigenesis, stimulated by *H. pylori* infection. Among these 25 genes, we focused on the CDK1 gene because (1) CDK1 is among the top 5 abnormal overexpression genes in the TCGA cohort; (2) CDK1 is a key member of the CDK family, (3) targeting CDKs has gained significant attention in the past few years,[30] and (4) its function in *H. pylori* infection-induced gastric tumorigenesis has not been explored yet. Herein, we found that Cdk1 expression was significantly induced in mice with *H. pylori* infection in our local and GEO: GSE13873 cohorts (Figure 1B). Furthermore, we detected a notable increase in CDK1 protein levels by performing immunofluorescence staining in *H. pylori* strain PMSS1-infected C57BL/6 (Figure 1C). We cultured gastric cancer (GC) cells alone or co-cultured with the wild-type cag+ *H. pylori* strain 7.13 or J166. The western blot and quantitative real-time PCR results showed that *H. pylori* infection significantly increased CDK1 mRNA and protein expression ($p < 0.01$; Figures 1D and 1E).

Using cell-cycle analysis, we have confirmed the classical function of CDK1 by showing a significant G2/M phase delay following the small interfering RNA (siRNA) knock down of CDK1 (Figure S1). Recent studies from our lab and others have demonstrated that overexpression of mitotic kinases in cancer such as Aurora kinases can have several

functions in cancer cells.[31–33] Therefore, we became interested in identifying functions for CDK1 in GC.

NF-κB binds to CDK1 promoter and regulates its expression

To accurately predict transcription factors (TFs) that can bind to the CDK1 promoter, we performed bioinformatics analysis with the TRRUST tool[34] by inputting DEGs of the CDK1-high expression group versus the CDK1-low expression group in the four indicated cohorts (Figure 2A). We finally identified 13 overlapping TFs, including two NF-κB relative TFs (NFkB1 and RELA) with high JASPAR scores (Figure 2B).[35] *H. pylori* infection activates NF-κB through both the canonical and the non-canonical pathways.[36] Therefore, we investigated whether *H. pylori* infection could upregulate CDK1 expression through activation of NF-κB. Western blot analysis data showed that *H. pylori* infection upregulated CDK1 and promoted induction of p-P65 (S536), confirming the activation of NF-κB (Figures 2C and 2D). To validate the pro-inflammatory effect of *H. pylori*, we evaluated the mRNA expression of inflammation-mediating cytokines in AGS cells infected with *H. pylori*. The quantitative real-time PCR data revealed that *H. pylori* infection significantly induced interleukin-1β (IL-1β) and TNF-α expression ($p < 0.01$; Figures S2A and S2B). To further prove that *H. pylori* infection leads to activation of NF-κB and increases expression of CDK1, we infected mice with mouse adapted *H. pylori* strain (PMSS1). Western blot analysis data showed an increase in CDK1 and p-P65 (S536) protein levels in the *H. pylori*-infected group compared with the non-infected controls (Figure 2E). The quantitative real-time PCR analysis of mice gastric tissues showed that infection with *H. pylori* resulted in significantly increased *Cdk1* mRNA expression compared with the uninfected controls ($p < 0.01$; Figure S2C). We next investigated if NF-κB regulates *CDK1* expression. We used transient expression of P65 in AGS and MKN28 cells, which led to a 2.5-fold induction of *CDK1* mRNA expression with a notable increase in CDK1 protein level (Figure 2F). We further verified these findings by using a TNF-α or NF-κB inhibitor. We treated GC cells with TNF-α or an NF-κB inhibitor (Bay 11-7082) to activate or inhibit NF-κB, respectively, and evaluated the *CDK1* mRNA and protein expression by quantitative real-time PCR and western blot analysis. We noticed that TNF-α significantly upregulated *CDK1* mRNA (Figure 2G) and protein (Figure 2H) levels in AGS and MKN28 cells. Collectively, these data suggest that NF-κB plays an important role in the transcriptional regulation of *CDK1* expression.

Our analysis of the *CDK1* promoter identified six possible NF-κB binding sites (Figure 3A). To characterize the NF-κB crucial elements for regulation on the *CDK1* promoter region, we designed 5 paired primers (P1–P5) containing all the putative binding sites (Figure 3B). To determine whether NF-κB regulates the expression of *CDK1* by directly binding to the promoter, we performed a chromatin immunoprecipitation (ChIP) assay by using a specific antibody against P65 to immunoprecipitate formaldehyde-fixed chromatin in AGS cells following transfection with pcDNA-p65 for 48 h or infection with *H. pylori* (7.13) for 24 h. We observed that P65 directly binds to the P1 region of the *CDK1* promoter and not to other regions ($p < 0.01$ and $p < 0.05$; Figure 3C). To further confirm the role of *H. pylori* in *CDK1* transcription regulation, AGS cells were transfected with CDK1-Luc luciferase reporter plasmid and co-cultured with *H. pylori* strain (7.13) alone or in combination

with Bay 11-7082 (NF-κB inhibitor). We found a significant induction of the CDK1-Luc reporter activity following *H. pylori* infection; the luciferase activity was completely blocked following NF-κB inhibition ($p < 0.01$; Figure 3D). To further validate NF-κB-P65 and *CDK1* promoter interaction, cells were transfected with a wild-type (WT)CDK1-Luc and P1 mutant luciferase construct (mutCDK1-Luc) reporter plasmid and then treated with TNF-α alone or in combination with Bay 11-7082 (Figures 3E and 3F). The promoter activity analysis showed that the relative luciferase activity of the WT-CDK1 significantly increased with TNF-α treatment ($p < 0.01$); treatment with Bay 11-7082 reversed these effects. In contrast, the relative luciferase activity of the mutCDK1 was not increased by TNF-α stimulation (Figures 3E and 3F). Notably, transient overexpression of P65 led to a dose-dependent increase of luciferase activity of the WT-CDK1, but not mutCDK1, reporter in AGS and MKN28 cells ($p < 0.01$; Figures 3G and 3H).

H. pylori infection activates CDK1-β-catenin axis

Recent studies have suggested non-mitotic functions of constitutively overexpressed mitotic proteins in cancer cells.[19,31–33] To explore the downstream signaling pathways regulated by CDK1 in GC in response to *H. pylori* infection, we performed gene set enrichment analysis (GSEA) using our cohort of mice with and without *H. pylori* infection. Earlier reports have shown activation of Wnt/β-catenin signaling by *H. pylori*, promoting cellular proliferation and transformation.[9,29,37] Our analysis demonstrated enrichment of several important oncogenic gene sets, including the Wnt signaling pathway in *H. pylori* infection samples (Figure 4A). Furthermore, Pearson's correlation test revealed a strong correlation between *CDK1* and *CTNNB1* expression levels in the GEO: GSE84433 cohort (Figure 4B). These findings suggested that β-catenin may be a critical downstream pathway in CDK1-high expressing cells in GC. To validate this hypothesis, we performed overexpression of CDK1 by using a CDK1 plasmid or tet-inducible system. We utilized the immortalized non-neoplastic gastric cells (GES1) or GC cells (AGS) that have absent to low endogenous CDK1 expression. We observed an increase in the β-catenin protein level following the overexpression of CDK1. The reverse effects were detected following the knock down of endogenously high levels of CDK1 in MKN45 cells (Figure 4C). Immunofluorescence analysis confirmed these findings where high levels of nuclear β-catenin were detected in AGS-CDK1 cells (Figure 4D). Furthermore, the TOP/FOP luciferase reporter data, as a measure of β-catenin/TCF transcription activity, demonstrated a significant induction of luciferase activity following overexpression of CDK1 ($p < 0.01$; Figure 4E). Opposite results were observed following the knock down of endogenous CDK1 ($p < 0.01$; Figure 4F). To confirm activation of β-catenin, the mRNA expression levels of β-catenin/TCF target genes were analyzed. The results demonstrated a significant increase in the mRNA expression levels of *AXIN2* ($p < 0.05$, and $p < 0.01$), and *CCDN1* ($p < 0.01$) in AGS and MKN28 cells with CDK1 overexpression compared with control (Figures 4G and 4H). In contrast, the knock down of endogenous CDK1 expression in MKN45 cells resulted in opposite effects ($p < 0.05$, and $p < 0.01$, respectively; Figures 4G and 4H). We also analyzed additional β-catenin/TCF target genes with ectopic CDK1 expression as well as with CDK1 knockdown with and without *H. pylori* infection in AGS and MKN28 cells. The results showed that CDK1 overexpression and *H. pylori* infection increased CCND1, AXIN2, *LEF1*, and *LGR5* mRNA levels (Figures S3A and S3B). Conversely, silencing CDK1 in MKN45 reversed

the results (Figure S3C). These findings suggest that CDK1 is required for β-catenin target genes.

It is important to understand cell signaling in a context relevant to the biology of the cancer type to improve our therapeutic strategies. To confirm that infection with *H. pylori* drives CDK1-β-catenin axis in gastric tumorigenesis, we cultured GES1, AGS, or MKN28 cells alone or co-cultured with *H. pylori* strain 7.13 or J166. Western blot results showed that *H. pylori* infection significantly increased CDK1 protein and phosphorylation of GSK-3β (S9) and β-catenin (S552) (Figures 5A and S4). The increase in phospho-GSK-3β (S9) level explains the increase in β-catenin levels as phospho-GSK-3β (S9) is inactive, allowing β-catenin accumulation and nuclear translocation. For *in vivo* validation, C57BL/6 mice were challenged with Brucella broth, as a negative control, or mouse adapted *H. pylori* strain PMSS1. Western blot analysis of mice gastric tissues showed that infection with *H. pylori* significantly increased CDK1 protein and phosphorylation of GSK-3β and β-catenin compared with uninfected controls (Figure 5B). Of note, the induction of phosphorylation of GSK-3β and β-catenin by *H. pylori* infection was abrogated by CDK1 knockdown (Figures 5C and 5D). Consistent with these results, *H. pylori* infection increased the TOP/FOP-flash reporter activities (6 h $p < 0.05$, 24 h $p < 0.01$) as a measure of β-catenin/TCF activity; this increase was abrogated by CDK1 knockdown (Figures 5E, 5F, and S5A). Similarly, *H pylori* infection upregulated the mRNA expression of β-catenin targets such as *AXIN2* and *CCND1* (Figures 5G, 5H, S5B, and S5C). Following these findings, immunofluorescence results demonstrated that *H. pylori* infection enhanced the nuclear accumulation of β-catenin (Figure 5I). Taken together, our results indicated that *H. pylori* infection activated the β-catenin signaling axis via induction of CDK1.

CDK1 regulates the GSK-3β/β-catenin pathway via protein-protein interaction

Next, we investigated if CDK1 can directly interact with GSK-3β and/or β-catenin. Using *in situ* proximity ligation assay (PLA) for endogenous CDK1 and GSK-3β or CDK1 and β-catenin, we detected a positive ligation, visualized by red signals for CDK1 and GSK-3β and CDK1 and β-catenin, indicative of their close proximity in AGS cells. These signals were not detected in the negative control as well as in PLA control using a single antibody (Figures S6A and S6B). We next utilized dual co-immunoprecipitation (coIP) to confirm the PLA findings and determine protein-protein interactions with the GSK-3β/β-catenin complex. We detected protein-protein interactions between CDK1, GSK-3β, and β-catenin (Figure S6C). Using *in vitro* kinase assay, we investigated whether CDK1 directly binds and phosphorylates GSK-3β. The results, using purified human recombinant CDK1 and GSK-3β proteins, confirmed that CDK1 can directly phosphorylate GSK-3β (S9) (Figure S6D). Notably, this effect was not seen using TFF1 recombinant protein (negative control). These results suggest that CDK1 regulates β-catenin via direct binding to and phosphorylating GSK3-β, rendering it inactive. This allows β-catenin to escape GSK-3β-mediated degradation, an essential step that promotes accumulation and activation of β-catenin in GC cells.

CDK1 promotes cell survival and expansion

Sustained activation of the β-catenin pathway provides cancer cells with stem-like properties including self-renewal and expansion capacities, associated with therapeutic resistance.[20,38] We therefore investigated the role of the CDK1-β-catenin axis in promoting these properties in GC cells. The GSEA indicated enrichment of several stem cell-relevant signatures[39,40] in GC samples with high-CDK1 expression across the TCGA and GEO datasets (Figure 6A). We also observed a correlation between the single-sample GSEA (ssGSEA) scores with β-catenin and its targets (Figure 6B). Furthermore, we tested the functions of CDK1 on cell expansion utilizing a spheroid culture assay. Spheroids with stable CDK1 shRNA knockdown showed less β-catenin staining than control cells (Figure 6C). CDK1 knockdown significantly decreased the size of spheroids ($p < 0.01$) compared with control groups (Figures 6D and 6E). Western blot analyses results showed that CDK1 knockdown significantly decreased phosphorylation of GSK-3β and β-catenin in MKN28 cells' spheroids (Figure 6F), confirming the role of CDK1 on β-catenin.

Silencing Cdk1 in mouse gastric mucosa abrogated *H. Pylori*-induced activation of β-catenin

Although *in vitro* assays are valuable tools to dissect mechanisms, it is critical to recapitulate the findings using *in vivo* models. To verify the role of CDK1 in β-catenin activation *in vivo*, we performed successful crossings of the $Cdk1^{flox/flox}$ mouse model (The Jackson Laboratory, Bar Harbor, ME, USA) with the $Krt19^{Cre}$ mouse model (the Jackson Laboratory) and obtained the $Krt19^{Cre}/Cdk1^{flox/flox}$ conditional CDK1 knockout mouse model. We established 4 groups (n = 5 per group): a control group, $Krt19^{Cre}/Cdk1^{floxl/flox}$, mice only infected with *H. pylori* (PMSS1), $Krt19^{Cre}/Cdk1^{flox/flox}$ receiving tamoxifen (TAM) treatment, and $Krt19^{Cre}Cdk1^{flox/flox}$ mice receiving TAM treatment and *H. pylori* infection (TAM + PMSS1) (Table S2). We developed organoids from these mice. Consistent with the *in vitro* observations, *H. pylori* infection increased the organoids' size, and CDK1 knockout significantly decreased the size of the organoids ($p < 0.01$; Figures 6G and 6H). The immunofluorescence staining of antral glandular stomach tissues demonstrated similar results as observed in cell lines: the *H. pylori* infection mice had higher CDK1 expression and increased numbers of nuclear β-catenin+ cells (Figure 7A). Using organoid tissue cultures from antral stomach regions of the four groups of mice, we determined that organoids from the *H. pylori* infection mice have higher CDK1 expression and β-catenin nuclear immunostaining than in the control and TAM + PMSS1 mice (Figure 7B). Concordant with these findings, we detected a significant increase in the mRNA expression levels of β-catenin target genes, *Ccnd1, Axin2, Lgr5*, and *Lef1* in the *H. pylori* (PMSS1)-infected mice, compared with the control and TAM + PMSS1 mice (Figure S7). In addition to *in vivo* and organoid data, silencing of CDK1 or its pharmacologic inhibition with dinaciclib or RO3306 attenuated sphere size and viability (Figures S8A–S8E). Consistently, pharmacologic CDK1 inhibition with dinaciclib or RO3306 decreased cell viability in multiple GC cell lines as measured by ATPGlo cell viability assay (IC50s are shown in Figures S8F and S8G).

High levels of CDK1 and β-catenin in human GC tissue samples

Immunohistochemistry (IHC) staining of CDK1 and β-catenin on human gastric tissue samples revealed weak immunostaining in the normal gastric mucosa (Figure 7C). Conversely, we observed strong immunostaining of CDK1 and β-catenin in adenocarcinomas (Figure 7C). Using a composite expression score (CES) as described in the STAR Methods, the IHC data indicated a significant increase in the expression of both CDK1 and β-catenin in gastric tumors ($p < 0.0$; Figure 7D). Moreover, a moderate correlation between CDK1 and β-cate-nin expression was revealed by Spearman's correlation analysis (coefficient $R = 0.41$, $p < 0.001$; Figure 7E). Our results from *in vitro*, mouse, and human models support the link between *H. pylori* infection, CDK1 expression, and β-catenin activation in gastric carcinogenesis. A diagram summarizing our findings is shown in Figure 7F.

DISCUSSION

GC ranks fifth for incidence and fourth for mortality worldwide. Despite efforts to eradicate *H. pylori*, the main risk factor, GC is responsible for over one million new cases in 2020, with an estimated 769,000 deaths.[1] Furthermore, most patients with GC present with advanced disease and have poor clinical out-comes.[41] Therefore, it is important to identify the molecular players in GC, a key step for improving our current diagnostic and therapeutic approaches. The objective of this study was to investigate whether *H. pylori* infection-induced inflammation could upregulate CDK1 expression, thereby facilitating gastric tumorigenesis.

H. pylori is classified by the World Health Organization as a class 1 carcinogen.[5] Chronic *H. pylori* infection and inflammation are the most established etiologic factors in the development of human GC.[6,7] We and others have shown that *H. pylori* infection of gastric mucosa creates a strong pro-inflammatory tumorigenic environment with activation of NF-κB, STAT3, β-catenin, and AKT.[9,10,42,43] This study reports a mechanism by which *H. pylori* infection promotes gastric tumorigenesis through activation of CDK1 expression. Our results link infection, inflammation, and activation of CDK1-dependent β-catenin signaling in gastric tumorigenesis.

Chronic inflammation is a key step in gastric tumorigenesis. Numerous pro-inflammatory stimuli activate NF-κB through the canonical or non-canonical pathways.[44,45] In this study, we reported that *H. pylori* infection mediated activation of pro-inflammatory NF-κB signaling associated with the increase in CDK1 level. Furthermore, we identified and confirmed several critical binding sites of NF-κB on the CDK1 promoter required for transcription regulation of CDK1 expression following *H. pylori* infection. We have previously shown that the $TFF1^{-/-}$ mouse model of gastric tumorigenesis and human GCs develop activation of NF-κB signaling in early stages.[10,46] NF-κB activation is a crucial mediator of inflammation-induced tumor growth and progression.[47] Our results show that *H. pylori*-mediated NF-κB activation increases CDK1 expression, strongly suggesting that CDK1 oncogenic functions may contribute to *H. pylori*-mediated gastric tumorigenesis. CDK1 is a cell-cycle regulator that drives cells through the G2 phase and mitosis. Accumulation of CDK1 was associated with cancer growth and a poor survival rate in

several cancer types.[19,48] Targeting CDK1 increased the efficacy of sorafenib treatment by targeting cancer stem cells in a preclinical model of hepatocellular carcinoma.[49] CDK1 inhibition induced caspase activation in pancreatic cell lines of pancreatic cancer.[50]

The equilibrium between cell migration, cell proliferation, and cell-cycle arrest is crucial for maintaining the homeostasis of the gastrointestinal epithelium. The canonical Wnt signaling pathway regulates proliferation, stem cell maintenance, and homeostasis in normal gastric mucosa in addition to its involvement in early embryogenesis.[20,22] β-catenin is a signaling transducer in the Wnt signaling pathway that serves as a transcriptional co-activator of TCF/LEF implicated in several cancer types.[22] Sustained activation of the β-catenin pathway provides cancer cells with stem-like properties and self-renewal capacity, regulating numerous aspects of cancers, including initiation, development, and progression. Although mutations in APC or CTNNB1 are a major cause of β-catenin nuclear accumulation in colorectal cancer,[24] these mutations generally occur in low frequencies (7% and 4%, respectively).[25] APC mutations are relatively more prevalent in the MSS/TP53+ subtype of GC than other molecular subtypes.[26] However, GCs demonstrate frequent β-catenin activation in the absence of causal mutations in *APC* or *CTNNB1*.[23,51]

Non-phosphorylated GSK-3β (S9) is kinase active and phosphorylates β-catenin (Ser33/37/Thr41), targeting it for E3 ligase-dependent ubiquitylation and subsequent proteasomal degradation.[52] We have demonstrated that activation of CDK1 by *H. pylori* infection induces binding to GSK-3β with phosphorylation at Ser9, rendering it kinase dead. Inactivation of GSK-3β via phosphorylation at Ser9 leads to accumulation of β-catenin with subsequent nuclear translocation and activation of the β-catenin/TCF transcription complex,[53] a critical step in gastric tumorigenesis. Using the $Krt19^{Cre}/Cdk1^{flox/flox}$ mouse model, we confirmed that silencing CDK1 abrogates the *H. pylori*-mediated nuclear accumulation of β-catenin. While earlier studies have shown activation of β-catenin by *H. pylori*,[6,9,12] our findings demonstrate a previously unknown role of CDK1 in this important process. Consistent with the role of β-catenin in cellular proliferation and expansion, gastric organoids and spheroids were fewer in number and smaller in size following silencing CDK1. Furthermore, we detected decreased cancer cell viability in response to CDK1 pharmacologic inhibition. Collectively, our results highlight an important role of CDK1 in GC and provide an explanation for non-mutational frequent activation of β-catenin under *H. pylori* infection in gastric tumorigenesis.

Given the importance of β-catenin in regulating numerous aspects of cancers, including the initiation, development, and progression of tumors, there have been several attempts to develop inhibitors along the WNT/β-catenin signaling pathway. However, most of the medications targeting Wnt/β-catenin signaling remain experimental and therapeutically poor and did not achieve satisfactory efficacy, specificity, and safety in clinical trials.[22] On the other hand, the use of dinaciclib, a small-molecule inhibitor of CDKs 1/2/5, showed encouraging effectiveness and favorable tolerability in a phase II clinical trial for myeloma[54] and a phase III clinical trial for chronic lymphocytic leukemia.[55] In lieu of our results, we suggest that targeting CDK1 and CDK1-dependent β-catenin signaling using CDK1 inhibitors could be an attractive therapeutic strategy whether as a single agent or, more likely, in combination with chemotherapeutics.

In summary, this study underscores a critical role of CDK1 overexpression in response to *H. pylori* infection during gastric tumorigenesis. CDK1 serves as a signaling bridge that links infection and inflammatory signaling to the activation of β-catenin, a critical transcription network co-activator in GC. This mechanism may explain the observed non-mutational activation of β-catenin in GC. The results suggest CDK1 as a molecular druggable vulnerability for the treatment of GC.

Limitations of the study

There are a number of limitations of the study. The present study did not investigate human tissues infected with *H. pylori* across the stages of gastric tumorigenesis. While the study showed the role of NF-κB in regulating the transcription of CDK1, it is possible that other TFs, activated by H. *pylori*, may also have an additive effect. Regulation of β-catenin is complex and heterogeneous. While CDK1 presents one mechanism regulating β-catenin, its precise contribution to the overall activation of β-catenin signaling versus other signaling pathways was not determined. The study did not investigate the efficacy of CDK1 inhibitors as single agents or in combination with standard-of-care chemotherapeutics in eliminating cancer cells.

STAR★METHODS

RESOURCE AVAILABILITY

Lead contact—Further information and requests for resources and reagents should be directed to and will be fulfilled by the lead contact, Wael El-Rifai (wxe45@miami.edu).

Materials availability—This study did not generate new unique reagents.

Data and code availability

- The original data within the paper will be available from the lead contact upon request.
- This paper does not report original code.
- Any additional information in this paper is available from the lead contact upon requests.

EXPERIMENTAL MODEL AND SUBJECT DETAILS

Animals—The 129S(B6N)-*Cdk1*^{tm1Eddy}/J (*Cdk1*$^{flox/flox}$) mice and *Krt19*$^{Cre/ERT}$ mice were purchased from The Jackson Laboratory (Bar Harbor, ME).[56,57] The *Cdk1*$^{flox/flox}$ and *Krt19*$^{Cre/ERT}$ were crossed to obtain the *Krt19*^{Cre}/*Cdk1*$^{flox/flox}$ mice. All animals were maintained in a pathogen-free state following the animal care committee-approved protocol of the University of Miami. Frozen and formalin-fixed paraffin-embedded stomach tissue samples were collected. All mice were of C57/B6/S129 mixed background. The age of mice was between 8-16 weeks. Male and female mice were included in all experiments. The remaining half of the stomach was snapfrozen and stored at −80°C for further use.

Cell culture and reagents—AGS cells were purchased from American Type Culture Collection (ATCC, Manassas, VA). MKN28 and MKN45 cells were obtained from the Riken Cell Bank (Tsukuba, Japan). AGS cells were cultured in F12 media (GIBCO, Carlsbad, CA). MKN28 and MKN45 cells were maintained in RPMI/1640 medium. All the mediums were supplemented with 10% fetal bovine serum (FBS, Invitrogen Life Technologies, Carlsbad, CA) and 1% penicillin/streptomycin (GIBCO). GES1 cells were a kind gift from Dr. Dawit Kidane-Mulat (The University of Texas-Austin, Austin, TX). GES1 cells were cultured in Dulbecco's modified Eagle's (GIBCO) medium. All cell lines were ascertained to conform to the original *in vitro* morphological characteristics. Cell lines were authenticated using short tandem repeat (STR) profiling (Genetica DNA Laboratories, Burlington, NC). All cell lines reported here have been tested and had shown to be free of mycoplasma (R&D Systems, Minneapolis, MN). Reagents and kits are listed in Table S3. Antibodies used in this study are listed in Table S4.

DNA plasmids, siRNA transfection, and shRNA lentivirus generation—Polyjet and LipoJet reagents were used for DNA and siRNA transfection. Respectively, following the manufacturer's instructions (Signagen Laboratories, Frederick, MD). Cdc2-HA was a gift from Dr. Sander van den Heuvel (Addgene plasmid # 1888). Control siRNA (universal negative control1) was purchased from Sigma-Aldrich (St. Louis, MO). The CDK1 siRNA (AM51331) was obtained from Thermo Fisher Scientific (Waltham, MA). The control shRNA and shCDK1 lentiviral plasmids were purchased from VectorBuilder (Guangzhou, China. https://en.vectorbuilder.com/). The control shRNA or CDK1shRNA lentiviral plasmids and 2nd Generation lentivirus packaging system (LV003, Abmgood) were co-transfected into HEK293T cells using the polyjet transfection reagent. Gastric cells were infected with the lentivirus (control shRNA or CDK1shRNAs) in the presence of 8 μg/mL of polybrene (TR-1003, Sigma-Aldrich). The transient transfection of pCMV4-p65 plasmid (purchased from Addgene)[58] or CDK1-Luciferase (VectorBuilder) was performed in 6-well plates. More details of DNA plasmids and shRNAs are listed in the Table S3. The siRNA and shRNA sequences are listed in Table S5.

METHOD DETAILS

Luciferase assay—The luciferase reporter assay was performed according to the manufacturer's protocol (Promega) as previously described.[27] Measurements using a Luminometer (BMG LABTECH) were conducted, following the manufacturer's protocol. β-galactosidase was used for normalization; each transfection was performed in triplicate.

Quantitative real-time PCR analysis—Total RNA was isolated by using the RNeasy Mini Kit (Qiagen, Valencia, CA)and 1 μg RNA was reverse transcribed by an iScript cDNA synthesis kit (Bio-Rad, Hercules, CA). The quantitative real-time PCR (qRT-PCR) was performed using a Bio-Rad CFX Connect Realtime System (Bio-Rad), with the threshold cycle number determined by Bio-Rad CFX manager software version 3.0. All primers were purchased from Integrated DNA Technologies (Table S5). The results of three independent experiments were subjected to statistical analysis. Fold change was calculated using the $_{\Delta\Delta}$C(t) method.[59] *HPRT1* was used as a normalization control.

Immunoprecipitation and western blotting—Cells were lysed with RIPA buffer supplemented with protease and phosphatase inhibitors (Santa Cruz, Dallas, TX). Immunoprecipitations of equivalent total protein amounts were performed overnight at 4°C by using a primary antibody previously bound to 40 μL of Protein A Dynabeads (Invitrogen, Carlsbad, CA) per sample. The beads were washed four times with a wash buffer. Proteins were separated on 12.5% SDS-PAGE and transferred to anImmobilon PVDF membrane (Millipore, Burlington, MA). Western blotting analysis was performed using standard methods. β-actin was used as the loading control. All blots were imaged using Bio-Rad ChemiDoc™ XRS+ System (Bio-Rad).

***In situ* proximity ligation assay (PLA) and immunofluorescence—**To demonstrate the proximity (<40 nm) between two different proteins in gastric cancer cells, PLA was performed by using Duo-link In Situ-Fluorescence kits according to the manufacturer's instructions (Sigma-Aldrich, St. Louis, MO). The slides were mounted with the mounting solution with DAPI. Each dot represents the proximity of two interacting proteins. Cell images were acquired using an Inverted laser-scanning LSM880-Airyscan (Zeiss, Thornwood, NY) confocal microscope.

Following cell fixation and permeabilization, immunofluorescence was performed using standard methods.[60] The cells were washed with cold PBS three times and incubated with both Alexa Fluor goat anti-rabbit IgG and Alexa Fluor goat anti-mouse IgG (1:800) (Invitrogen) at room temperature for 1.5 h. Cell images were acquired using an Inverted laser-scanning LSM880-Airyscan (Zeiss, Thornwood, NY) confocal microscope.

Chromatin immunoprecipitation (ChIP)—The ChIP analysis was performed according to the manufacturer's instructions using ChIP-IT Express Enzymatic and ChIP-IT High Sensitivity kit (Active Motif Inc, Carlsbad, CA). Quantitative real-time PCR was used to analyze the binding of NF-κB to the promoter of the CDK1 target gene. Primers for ChIP qRT-PCR were provided in Table S5.

Infection of mice with H. pylori—All animals studied were carried out following the recommendations from the Guide for the Care and Use of Laboratory Animals of the National Institutes of Health. The Institutional Animal Care and Use Committee (IACUC) at the University of Miami approved all protocols and efforts made to minimize animal suffering. C57BL/6 mice were purchased from Charles River Laboratories and divided into two groups (10 per group) for infection with *H. pylori* or control (broth). At the age of 8–10 weeks, the $Krt19^{Cre/Ert}/Cdk1^{flox/flox}$ mice were divided into four group (4–5 per group) for treatment with or without Tamoxifen (50 mg/kg, IP) for 10 days. For infection with *H. pylori*, mice were orogastrically challenged with Brucella broth, as an uninfected control, or with the mouse-adapted wild-type *H. pylori* strain PMSS1 (10^9 CFU/mouse) at the age of 10–12 weeks.[61] Mice were euthanized after 1–2 months post challenge and gastric tissues were harvested for western blot and real-time PCR analyses.

Tumor spheroid culture—MKN28 control and CDK1 stable knockdown cells were seeded into ultra-low attachment 6-well dishes (Corning, Corning, NY) and cultured in serum-free DMEM/F12 supplemented with 20 ng/mL epidermal growth factor (EGF),

10 ng/mL basic fibroblast growth factor (bFGF), 2% B-27 (Life Technologies, Carlsbad, CA). The culture medium was changed every three days. The diameter and number of tumor spheres in three random 100x magnifications fields were calculated under All-in-one Fluorescence Microscope (BZ-X700, Keyence Corp, Atlanta, GA) using the bright field mode.

H. pylori strains—*H. pylori* cagA$^+$ strains (7.13 and J166) were used for cell lines infection. In addition, Rodent-adapted *cag*$^+$ *H. pylori* strain PMSS1 was used for *in vivo* mouse experiments. *H. pylori* bacteria were cultured on trypticase soy agar with 5% sheep blood agar plates (BD Biosciences, Franklin Lakes, NJ) as previously described.[62] *H. pylori* strains were then cultured in Brucella broth (BD Biosciences) supplemented with 10% fetal bovine serum (Atlanta Biologicals, Flowery Branch, GA) for 16 to 18 hours at 37°C with 10% CO_2. For *in vitro* studies, the bacteria were co-cultured with gastric epithelial cells at a multiplicity of infection (MOI) of 100:1.

Gastric organoids—The mouse stomach was cut into 2–3 mm pieces and then incubated in 5 mM EDTA for 30 minutes, with shaking at 37°C. The cell suspension passed through 40 μm cell strainers 2 times. After centrifuging at 1200 RPM for 5 minutes, the pellet was suspended in 50 μL Matrigel (BD Biosciences) and plated in pre-warmed 24-well plates. The 24-well plate was placed in a CO_2 incubator for 20 minutes to allow a complete polymerization of the Matrigel, 500 μL mouse basal medium (STEMCELL, Cambridge, MA) was overlaid. Organoids were collected after 14 days, fixed in 4% paraformaldehyde for 20 min, washed in 1× PBS, and re-suspended in 30 μL Histo-gel (Richard-Allan, White Plains, NY). The histo-gel was placed into a cassette and fixed in 70% ethanol. Paraffin-embedded organoids were pretreated at 65°C for 90 min, followed by deparaffinization using standard procedures.[60] Antigen retrieval was performed using Tris EDTA Buffer (Genemed, Torrance, CA). Slides were then incubated for primary antibody overnight at 4°C, and further incubated with both Alexa Fluor goat anti-rabbit IgG and Alexa Fluor goat anti-mouse IgG (1:800) (Invitrogen) at room temperature for 2 h. Images were acquired using an inverted laser-scanning LSM880-Airyscan (Zeiss, Thornwood, NY) confocal microscope.

Gene set enrichment analysis (GSEA) and single-sample gene set enrichment analysis (ssGSEA)—The reference gene sets were obtained based on the literature[39,40] or downloaded from MSigDB (https://www.gsea-msigdb.org/gsea/index.jsp). The “limma” package was performed to identify the differential expression genes (DEGs) of CDK1 high expression samples compared with CDK1 low expression samples. The Normalization Enrichment Score (NES) and the false discovery rate (FDR) of each gene set were calculated using the “cluster Profiler”(v3.12.0) package.[63] Each gene set was considered significant when the FDR was less than 25%. The Single-Sample Gene Set Enrichment Analysis (ssGSEA) program[64] was used to quantify the enrichment scores of each stem cell’s relative signature.

Public gene expression data analysis—The TCGA gastric cancer cohort was downloaded from NCI (https://portal.gdc.cancer.gov/) to identify the significant genes

and analyze their expression in gastric cancer. In addition, a series of human gastric cancer datasets (GSE122401, GSE84433, GSE54129) and mouse datasets (GSE13873) were obtained from GEO DataSets (https://www.ncbi.nlm.nih.gov/gds/). The mean value of probes was utilized as the gene expression when a gene has multiple probes. All data were analyzed using R software (R 3.6.1; https://www.r-project.org/).

Immunohistochemistry and RNA analysis—Human de-identified gastric tissue samples were obtained from Fujian Medical University Union Hospital (FJMUUH, Fuzhou, China). 216 assessable cases of tumor tissue microarrays (TMA) and their adjacent non-tumor tissues were used for immunohistochemistry. Immunohistochemistry (IHC) staining was performed as described previously,[65] using the rabbit anti-human CDK1 antibody (ab133327, Abcam, Waltham, MA) and β-catenin antibody (37447, Cell signaling, Danvers, MA). All tissue samples were collected, coded, and de-identified following Institutional Review Board-approved protocols. Images were taken by Olympus FSX100 microscope (Olympus, Japan) at 4× and 40× magnification. The scoring criteria were described as previously.[65] Five fields were randomly selected to assess the intensity and percentage of positive cells in each slide. The final score for each slide was calculated as the formula: the proportion score × the intensity score (range from 0 to 9 totally).

36 cases of fresh tumor tissues and their adjacent non-tumor tissues were collected for whole-transcriptome sequencing. Trizol (Invitrogen) was utilized to lyse all tissues, and RNA sequencing was performed using gene expression arrays following MIAME guidelines (Shanghai, China). RNA was extracted from 14 mice's stomachs as described,[66] the RNA samples were analyzed using the Illumina HiSeq 2500 platform, and the Illumina (San Diego, CA)Tru-seq RNA sample prep kit was used for library preparation. Informed consent was obtained from all the subjects and all experimental protocols using human specimens have been approved by the institutional review committee of FJMUUH.

QUANTIFICATION AND STATISTICAL ANALYSIS

All experiments were repeated in three independent experiments, and a means ± SD was used. The SPSS statistical package for Windows Version 16 (SPSS, Chicago, IL, USA) was used for the Pearson Chi-square test and the multi-variant Cox regression analysis. Statistical significance of the *in vitro* and *in vivo* studies was analyzed by the one-way ANOVA, 2-tailed Student's t-test, and Pearson's Correlation Coefficient analysis using the GraphPad Prism 8 software (GraphPad Software, Inc, San Diego, CA, USA). Significant differences are described in the figure legends as $p < 0.05$ or $p < 0.01$.

Supplementary Material

Refer to Web version on PubMed Central for supplementary material.

ACKNOWLEDGMENTS

We would like to thank Ms. Carla Otiniano for assisting in the preparation of this manuscript. This study was supported by US NIH funding (R01CA249949) and Department of Veterans Affairs awards (1IK6BX003787 and I01BX001179). The use of shared resources was supported by the National Cancer Institute-funded Sylvester Comprehensive Cancer Center P30CA240139. This work's content is solely the responsibility of the authors. It

does not necessarily represent the official views of the Department of Veterans Affairs, the NIH, or the University of Miami.

REFERENCES

1. Sung H, Ferlay J, Siegel RL, Laversanne M, Soerjomataram I, Jemal A, and Bray F (2021). Global cancer statistics 2020: GLOBOCAN estimates of incidence and mortality worldwide for 36 cancers in 185 countries. CA Cancer J. Clin 71, 209–249. 10.3322/caac.21660. [PubMed: 33538338]
2. Jim MA, Pinheiro PS, Carreira H, Espey DK, Wiggins CL, and Weir HK (2017). Stomach cancer survival in the United States by race and stage (2001-2009): findings from the CONCORD-2 study. Cancer 123 (Suppl 24), 4994–5013. 10.1002/cncr.30881. [PubMed: 29205310]
3. Diaconu S, Predescu A, Moldoveanu A, Pop CS, and Fierbinteanu-Braticevici C (2017). Helicobacter pylori infection: old and new. J. Med. Life 10, 112–117. [PubMed: 28616085]
4. Savoldi A, Carrara E, Graham DY, Conti M, and Tacconelli E (2018). Prevalence of antibiotic resistance in Helicobacter pylori: a systematic review and meta-analysis in world health organization regions. Gastroenterology 155, 1372–1382.e17. 10.1053/j.gastro.2018.07.007. [PubMed: 29990487]
5. Author Anonymous. (1994). Infection with Helicobacter pylori. IARC Monogr. Eval. Carcinog. Risks Hum 61, 177–240. [PubMed: 7715070]
6. Polk DB, and Peek RM Jr. (2010). Helicobacter pylori: gastric cancer and beyond. Nat. Rev. Cancer 10, 403–414. [PubMed: 20495574]
7. Fox JG, and Wang TC (2007). Inflammation, atrophy, and gastric cancer. J. Clin. Invest 117, 60–69. 10.1172/JCI30111. [PubMed: 17200707]
8. Peek RM Jr., and Blaser MJ (2002). Helicobacter pylori and gastrointestinal tract adenocarcinomas. Nat. Rev. Cancer 2, 28–37. 10.1038/nrc703. [PubMed: 11902583]
9. Soutto M, Romero-Gallo J, Krishna U, Piazuelo MB, Washington MK, Belkhiri A, Peek RM Jr., and El-Rifai W (2015). Loss of TFF1 promotes Helicobacter pylori-induced beta-catenin activation and gastric tumorigenesis. Oncotarget 6, 17911–17922. 10.18632/oncotarget.3772. [PubMed: 25980439]
10. Zhu S, Soutto M, Chen Z, Peng D, Romero-Gallo J, Krishna US, Belkhiri A, Washington MK, Peek R, and El-Rifai W (2017). Helicobacter pylori-induced cell death is counteracted by NF-kappaB-mediated transcription of DARPP-32. Gut 66, 761–762. 10.1136/gutjnl-2016-312141.
11. Correa P (1988). A human model of gastric carcinogenesis. Cancer Res. 48, 3554–3560. [PubMed: 3288329]
12. Ito N, Tsujimoto H, Ueno H, Xie Q, and Shinomiya N (2020). Helicobacter pylori-mediated immunity and signaling transduction in gastric cancer. J. Clin. Med 9, 3699. 10.3390/jcm9113699. [PubMed: 33217986]
13. Taniguchi K, and Karin M (2018). NF-kappaB, inflammation, immunity and cancer: coming of age. Nat. Rev. Immunol 18, 309–324. 10.1038/nri.2017.142. [PubMed: 29379212]
14. Xie XK, Xu ZK, Xu K, and Xiao YX (2020). DUSP19 mediates spinal cord injury-induced apoptosis and inflammation in mouse primary microglia cells via the NF-kB signaling pathway. Neurol. Res 42, 31–38. 10.1080/01616412.2019.1685068. [PubMed: 31813339]
15. Liu T, Zhang L, Joo D, and Sun SC (2017). NF-kappaB signaling in inflammation. Signal Transduct. Target. Ther 2, 17023-. 10.1038/sigtrans.2017.23. [PubMed: 29158945]
16. Safa AR (2020). Epithelial-mesenchymal transition: a hallmark in pancreatic cancer stem cell migration, metastasis formation, and drug resistance. J. Cancer Metastasis Treat 6, 36. 10.20517/2394-4722.2020.55. [PubMed: 34841087]
17. Diril MK, Ratnacaram CK, Padmakumar VC, Du T, Wasser M, Coppola V, Tessarollo L, and Kaldis P (2012). Cyclin-dependent kinase 1 (Cdk1) is essential for cell division and suppression of DNA re-replication but not for liver regeneration. Proc. Natl. Acad. Sci. USA 109, 3826–3831. 10.1073/pnas.1115201109. [PubMed: 22355113]
18. Castedo M, Perfettini JL, Roumier T, and Kroemer G (2002). Cyclin-dependent kinase-1: linking apoptosis to cell cycle and mitotic catastrophe. Cell Death Differ. 9, 1287–1293. 10.1038/sj.cdd.4401130. [PubMed: 12478465]

19. Yang W, Cho H, Shin HY, Chung JY, Kang ES, Lee EJ, and Kim JH (2016). Accumulation of cytoplasmic Cdk1 is associated with cancer growth and survival rate in epithelial ovarian cancer. Oncotarget 7, 49481–49497. 10.18632/oncotarget.10373. [PubMed: 27385216]
20. Zhan T, Rindtorff N, and Boutros M (2017). Wnt signaling in cancer. Oncogene 36, 1461–1473. 10.1038/onc.2016.304. [PubMed: 27617575]
21. MacDonald BT, and He X (2012). Frizzled and LRP5/6 receptors for Wnt/beta-catenin signaling. Cold Spring Harb. Perspect. Biol 4, a007880. 10.1101/cshperspect.a007880. [PubMed: 23209147]
22. Yu F, Yu C, Li F, Zuo Y, Wang Y, Yao L, Wu C, Wang C, and Ye L (2021). Wnt/beta-catenin signaling in cancers and targeted therapies. Signal Transduct. Target. Ther 6, 307. 10.1038/s41392-021-00701-5. [PubMed: 34456337]
23. Song X, Xin N, Wang W, and Zhao C (2015). Wnt/beta-catenin, an oncogenic pathway targeted by H. pylori in gastric carcinogenesis. Oncotarget 6, 35579–35588. 10.18632/oncotarget.5758. [PubMed: 26417932]
24. Schell MJ, Yang M, Teer JK, Lo FY, Madan A, Coppola D, Monteiro ANA, Nebozhyn MV, Yue B, Loboda A, et al. (2016). A multigene mutation classification of 468 colorectal cancers reveals a prognostic role for APC. Nat. Commun 7, 11743. 10.1038/ncomms11743. [PubMed: 27302369]
25. Cancer Genome Atlas Research Network (2014). Comprehensive molecular characterization of gastric adenocarcinoma. Nature 513, 202–209. 10.1038/nature13480. [PubMed: 25079317]
26. Cristescu R, Lee J, Nebozhyn M, Kim KM, Ting JC, Wong SS, Liu J, Yue YG, Wang J, Yu K, et al. (2015). Molecular analysis of gastric cancer identifies subtypes associated with distinct clinical outcomes. Nat. Med 21, 449–456. 10.1038/nm.3850. [PubMed: 25894828]
27. Soutto M, Peng D, Katsha A, Chen Z, Piazuelo MB, Washington MK, Belkhiri A, Correa P, and El-Rifai W (2015). Activation of beta-catenin signalling by TFF1 loss promotes cell proliferation and gastric tumorigenesis. Gut 64, 1028–1039. 10.1136/gutjnl-2014-307191. [PubMed: 25107557]
28. Koushyar S, Powell AG, Vincan E, and Phesse TJ (2020). Targeting Wnt signaling for the treatment of gastric cancer. Int. J. Mol. Sci 21, 3927. 10.3390/ijms21113927. [PubMed: 32486243]
29. Cao L, Zhu S, Lu H, Soutto M, Bhat N, Chen Z, Peng D, Lin J, Lu J, Li P, et al. (2022). Helicobacter pylori-induced RASAL2 through activation of nuclear factor-kappaB promotes gastric tumorigenesis via beta-catenin signaling axis. Gastroenterology 162, 1716–1731.e17. 10.1053/j.gastro.2022.01.046. [PubMed: 35134322]
30. Hossain DMS, Javaid S, Cai M, Zhang C, Sawant A, Hinton M, Sathe M, Grein J, Blumenschein W, Pinheiro EM, and Chackerian A (2018). Dinaciclib induces immunogenic cell death and enhances anti-PD1-mediated tumor suppression. J. Clin. Invest 128, 644–654. 10.1172/JCI94586. [PubMed: 29337311]
31. Dar AA, Belkhiri A, and El-Rifai W (2009). The aurora kinase A regulates GSK-3beta in gastric cancer cells. Oncogene 28, 866–875. 10.1038/onc.2008.434. [PubMed: 19060929]
32. Katsha A, Wang L, Arras J, Omar OM, Ecsedy J, Belkhiri A, and El-Rifai W (2017). Activation of EIF4E by Aurora kinase A depicts a novel druggable axis in everolimus resistant cancer cells. Clin. Cancer Res 23, 3756–3768. 10.1158/1078-0432.CCR-16-2141. [PubMed: 28073841]
33. Wang-Bishop L, Chen Z, Gomaa A, Lockhart AC, Salaria S, Wang J, Lewis KB, Ecsedy J, Washington K, Beauchamp RD, and El-Rifai W (2019). Inhibition of AURKA reduces proliferation and survival of gastrointestinal cancer cells with activated KRAS by preventing activation of RPS6KB1. Gastroenterology 156, 662–675.e7. 10.1053/j.gastro.2018.10.030. [PubMed: 30342037]
34. Han H, Cho JW, Lee S, Yun A, Kim H, Bae D, Yang S, Kim CY, Lee M, Kim E, et al. (2018). TRRUST v2: an expanded reference database of human and mouse transcriptional regulatory interactions. Nucleic Acids Res. 46, D380–D386. 10.1093/nar/gkx1013. [PubMed: 29087512]
35. Fornes O, Castro-Mondragon JA, Khan A, van der Lee R, Zhang X, Richmond PA, Modi BP, Correard S, Gheorghe M, Baranašić D, et al. (2020). JASPAR 2020: update of the open-access database of transcription factor binding profiles. Nucleic Acids Res. 48, D87–D92. 10.1093/nar/gkz1001. [PubMed: 31701148]
36. Lamb A, and Chen LF (2010). The many roads traveled by Helicobacter pylori to NFkappaB activation. Gut Microb. 1, 109–113. 10.4161/gmic.1.2.11587.

37. Franco AT, Israel DA, Washington MK, Krishna U, Fox JG, Rogers AB, Neish AS, Collier-Hyams L, Perez-Perez GI, Hata-keyama M, et al. (2005). Activation of beta-catenin by carcinogenic Helicobacter pylori. Proc. Natl. Acad. Sci. USA 102, 10646–10651. 10.1073/pnas.0504927102. [PubMed: 16027366]
38. Kim MJ, Huang Y, and Park JI (2020). Targeting Wnt signaling for gastrointestinal cancer therapy: present and evolving views. Cancers 12, 3638. 10.3390/cancers12123638. [PubMed: 33291655]
39. Miranda A, Hamilton PT, Zhang AW, Pattnaik S, Becht E, Mezheyeuski A, Bruun J, Micke P, de Reynies A, and Nelson BH (2019). Cancer stemness, intratumoral heterogeneity, and immune response across cancers. Proc. Natl. Acad. Sci. USA 116, 9020–9029. 10.1073/pnas.1818210116. [PubMed: 30996127]
40. Malta TM, Sokolov A, Gentles AJ, Burzykowski T, Poisson L, Weinstein JN, Kamińska B, Huelsken J, Omberg L, Gevaert O, et al. (2018). Machine learning identifies stemness features associated with oncogenic dedifferentiation. Cell 173, 338–354.e15. 10.1016/j.cell.2018.03.034. [PubMed: 29625051]
41. Siegel RL, Miller KD, Fuchs HE, and Jemal A (2021). Cancer statistics, 2021. CA Cancer J. Clin 71, 7–33. 10.3322/caac.21654. [PubMed: 33433946]
42. Bhardwaj V, Noto JM, Wei J, Andl C, El-Rifai W, Peek RM, and Zaika AI (2015). Helicobacter pylori bacteria alter the p53 stress response via ERK-HDM2 pathway. Oncotarget 6, 1531–1543. [PubMed: 25605238]
43. Suarez G, and Peek RM Jr. (2014). Helicobacter pylori: expect the unexpected. Mol. Microbiol 91, 858–861. 10.1111/mmi.12532. [PubMed: 24471732]
44. Senftleben U, Cao Y, Xiao G, Greten FR, Krähn G, Bonizzi G, Chen Y, Hu Y, Fong A, Sun SC, and Karin M (2001). Activation by IKKalpha of a second, evolutionary conserved, NF-kappa B signaling pathway. Science 293, 1495–1499. 10.1126/science.1062677. [PubMed: 11520989]
45. Ghosh S, and Karin M (2002). Missing pieces in the NF-kappaB puzzle. Cell 109, S81–S96. [PubMed: 11983155]
46. Soutto M, Belkhiri A, Piazuelo MB, Schneider BG, Peng D, Jiang A, Washington MK, Kokoye Y, Crowe SE, Zaika A, et al. (2011). Loss of TFF1 is associated with activation of NF-kappaB-mediated inflammation and gastric neoplasia in mice and humans. J. Clin. Invest 121, 1753–1767. 10.1172/JCI43922. [PubMed: 21490402]
47. Romieu-Mourez R, Landesman-Bollag E, Seldin DC, Traish AM, Mercurio F, and Sonenshein GE (2001). Roles of IKK kinases and protein kinase CK2 in activation of nuclear factor-kappaB in breast cancer. Cancer Res. 61, 3810–3818. [PubMed: 11325857]
48. Luo Y, Wu Y, Peng Y, Liu X, Bie J, and Li S (2016). Systematic analysis to identify a key role of CDK1 in mediating gene interaction networks in cervical cancer development. Ir. J. Med. Sci 185, 231–239. 10.1007/s11845-015-1283-8. [PubMed: 25786624]
49. Wu CX, Wang XQ, Chok SH, Man K, Tsang SHY, Chan ACY, Ma KW, Xia W, and Cheung TT (2018). Blocking CDK1/PDK1/beta-Catenin signaling by CDK1 inhibitor RO3306 increased the efficacy of sorafenib treatment by targeting cancer stem cells in a preclinical model of hepatocellular carcinoma. Theranostics 8, 3737–3750. 10.7150/thno.25487. [PubMed: 30083256]
50. Huang J, Chen P, Liu K, Liu J, Zhou B, Wu R, Peng Q, Liu ZX, Li C, Kroemer G, et al. (2021). CDK1/2/5 inhibition overcomes IFNG-mediated adaptive immune resistance in pancreatic cancer. Gut 70, 890–899. 10.1136/gutjnl-2019-320441. [PubMed: 32816920]
51. Woo DK, Kim HS, Lee HS, Kang YH, Yang HK, and Kim WH (2001). Altered expression and mutation of beta-catenin gene in gastric carcinomas and cell lines. Int. J. Cancer 95, 108–113. 10.1002/1097-0215(20010320)95:2<108::aid-ijc1019>3.0.co;2-#. [PubMed: 11241321]
52. Wang XQ, Lo CM, Chen L, Ngan ESW, Xu A, and Poon RY (2017). CDK1-PDK1-PI3K/Akt signaling pathway regulates embryonic and induced pluripotency. Cell Death Differ. 24, 38–48. 10.1038/cdd.2016.84. [PubMed: 27636107]
53. Wu D, and Pan W (2010). GSK3: a multifaceted kinase in Wnt signaling. Trends Biochem. Sci 35, 161–168. 10.1016/j.tibs.2009.10.002. [PubMed: 19884009]
54. Kumar SK, LaPlant B, Chng WJ, Zonder J, Callander N, Fonseca R, Fruth B, Roy V, Erlichman C, and Stewart AK; Mayo Phase 2 Consortium (2015). Dinaciclib, a novel CDK inhibitor,

demonstrates encouraging single-agent activity in patients with relapsed multiple myeloma. Blood 125, 443–448. 10.1182/blood-2014-05-573741. [PubMed: 25395429]

55. Ghia P, Scarfò L, Perez S, Pathiraja K, Derosier M, Small K, McCrary Sisk C, and Patton N (2017). Efficacy and safety of dinaciclib vs ofatumumab in patients with relapsed/refractory chronic lymphocytic leukemia. Blood 129, 1876–1878. 10.1182/blood-2016-10-748210. [PubMed: 28126927]
56. Fienberg AA, Hiroi N, Mermelstein PG, Song W, Snyder GL, Nishi A, Cheramy A, O'Callaghan JP, Miller DB, Cole DG, et al. (1998). DARPP-32: regulator of the efficacy of dopaminergic neurotransmission. Science 281, 838–842. [PubMed: 9694658]
57. Means AL, Xu Y, Zhao A, Ray KC, and Gu G (2008). A CK19(CreERT) knockin mouse line allows for conditional DNA recombination in epithelial cells in multiple endodermal organs. Genesis 46, 318–323. 10.1002/dvg.20397. [PubMed: 18543299]
58. Ballard DW, Dixon EP, Peffer NJ, Bogerd H, Doerre S, Stein B, and Greene WC (1992). The 65-kDa subunit of human NF-kappa B functions as a potent transcriptional activator and a target for v-Rel-mediated repression. Proc. Natl. Acad. Sci. USA 89, 1875–1879. 10.1073/pnas.89.5.1875. [PubMed: 1542686]
59. Pfaffl MW (2001). A new mathematical model for relative quantification in real-time RT-PCR. Nucleic Acids Res. 29, e45. [PubMed: 11328886]
60. Zhu S, Soutto M, Chen Z, Blanca Piazuelo M, Kay Washington M, Belkhiri A, Zaika A, Peng D, and El-Rifai W (2019). Activation of IGF1R by DARPP-32 promotes STAT3 signaling in gastric cancer cells. Oncogene 38, 5805–5816. 10.1038/s41388-019-0843-1. [PubMed: 31235784]
61. Noto JM, Khizanishvili T, Chaturvedi R, Piazuelo MB, Romero-Gallo J, Delgado AG, Khurana SS, Sierra JC, Krishna US, Suarez G, et al. (2013). Helicobacter pylori promotes the expression of Kruppel-like factor 5, a mediator of carcinogenesis, in vitro and in vivo. PLoS One 8, e54344. 10.1371/journal.pone.0054344. [PubMed: 23372710]
62. Franco AT, Johnston E, Krishna U, Yamaoka Y, Israel DA, Nagy TA, Wroblewski LE, Piazuelo MB, Correa P, and Peek RM Jr. (2008). Regulation of gastric carcinogenesis by Helicobacter pylori virulence factors. Cancer Res. 68, 379–387. 10.1158/0008-5472.CAN-07-0824. [PubMed: 18199531]
63. Yu G, Wang LG, Han Y, and He QY (2012). clusterProfiler: an R package for comparing biological themes among gene clusters. OMICS 16, 284–287. 10.1089/omi.2011.0118. [PubMed: 22455463]
64. Barbie DA, Tamayo P, Boehm JS, Kim SY, Moody SE, Dunn IF, Schinzel AC, Sandy P, Meylan E, Scholl C, et al. (2009). Systematic RNA interference reveals that oncogenic KRAS-driven cancers require TBK1. Nature 462, 108–112. 10.1038/nature08460. [PubMed: 19847166]
65. Wang JB, Li P, Liu XL, Zheng QL, Ma YB, Zhao YJ, Xie JW, Lin JX, Lu J, Chen QY, et al. (2020). An immune checkpoint score system for prognostic evaluation and adjuvant chemotherapy selection in gastric cancer. Nat. Commun 11, 6352. 10.1038/s41467-020-20260-7. [PubMed: 33311518]
66. Chen Z, Li Z, Soutto M, Wang W, Piazuelo MB, Zhu S, Guo Y, Maturana MJ, Corvalan AH, Chen X, et al. (2019). Integrated analysis of mouse and human gastric neoplasms identifies conserved microRNA networks in gastric carcinogenesis. Gastroenterology 156, 1127–1139.e8. 10.1053/j.gastro.2018.11.052. [PubMed: 30502323]

Highlights

- Infection with *H. pylori* is the main risk factor for gastric tumorigenesis
- *H. pylori* infection induces CDK1 expression via an NF-κB-dependent transcription
- CDK1 promotes activation of β-catenin signaling and cellular expansion

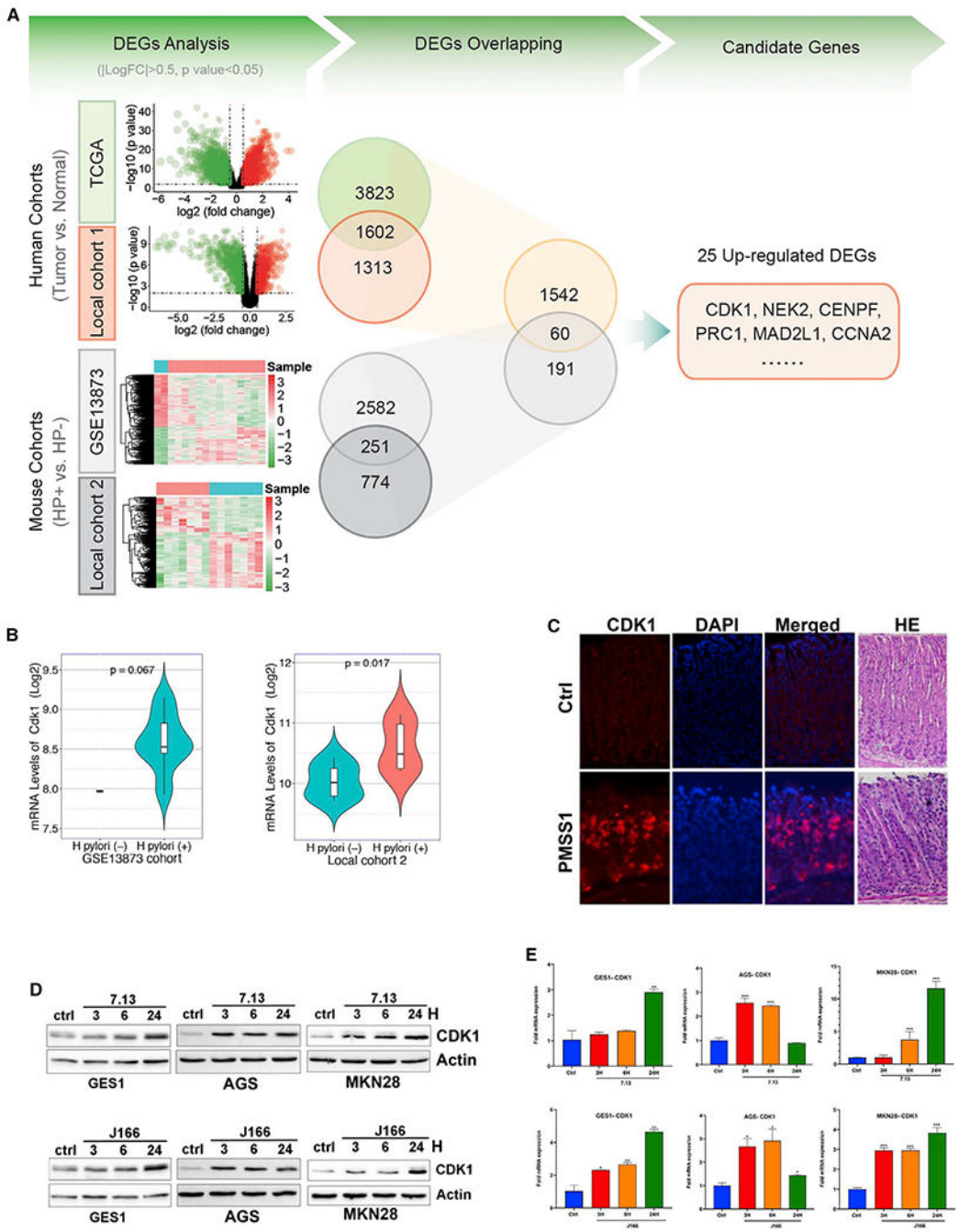

Figure 1. CDK1 is overexpressed in gastric cancer

(A) Analyses of two Gene Expression Omnibus (GEO) datasets from tumor versus normal (TN) and *H. pylori* (HP) cohorts. Hierarchical clustering heatmap and volcano plots of significant differentially expressed genes (DEGs) are shown in DEG analysis. Overlapping TN cohorts and HP cohorts initially identified 60 DEGs.

(B) The mRNA expression levels of CDK1 were examined in the GEO datasets and our local cohort with *H. pylori* infection.

(C) Immunofluorescence staining for CDK1 (red) was performed in mice orogastrically challenged with Brucella broth or PMSS1, and representative images are shown. H&E staining of representative histological features of gastric mucosa mice.
(D and E) Western blot and quantitative real-time analysis of CDK1 in GES1, AGS, and MKN28 cells following *H. pylori* infection.
Experiments were performed in triplicates. *$p < 0.05$ and **$p < 0.01$.

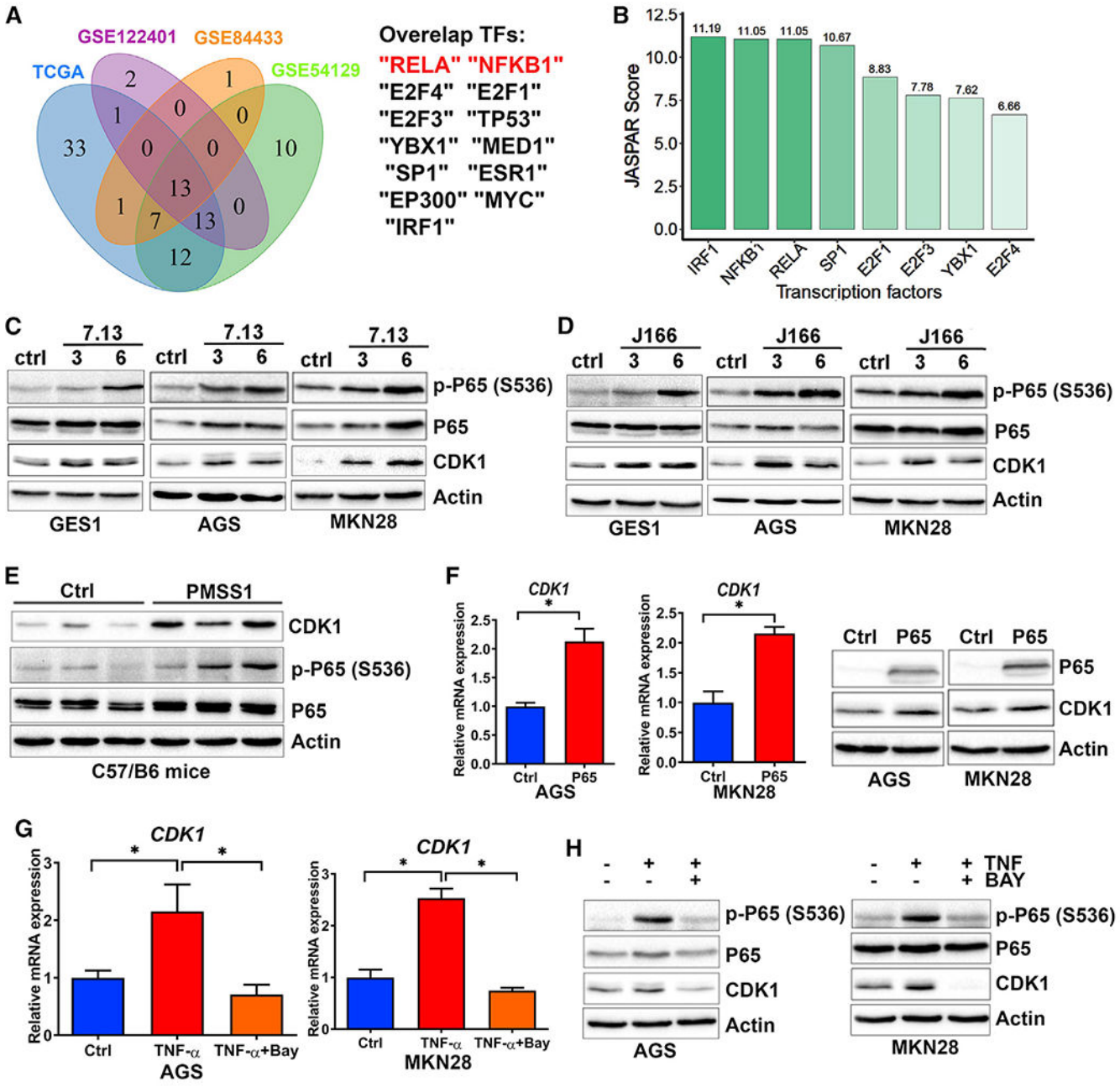

Figure 2. Activation of NF-κB-P65 upregulates CDK1 expression

(A) The transcription factor binding sites were predicted by the PROMO website using a 2,000-bp conserved segment of the CDK1 promoter.

(B) A list of putative transcriptional factors with higher JASPAR scores in human and mouse CDK1 promoters.

(C and D) Western blot analyses of p-P65 (S536), P65, and CDK1 in GES1, AGS, and MKN28 cells following *H. pylori* infection (7.13 and J166).

(E) The western blot analyses of p-P65 (S536), P65, and CDK1 were performed in mice orogastrically challenged with Brucella broth or with PMSS1.

(F) The immunoblot analyses and quantitative real-time PCR were performed to determine CDK1 expression in AGS and MKN28 cells transiently transfected with P65 or empty vector.

(G and H) The immunoblot analyses and quantitative real-time PCR of p-P65 (S536), P65, and CDK1 were performed in AGS and MKN28 cells following TNF-α and Bay 11-7082 treatment.

Experiments were performed in triplicates. *$p < 0.05$.

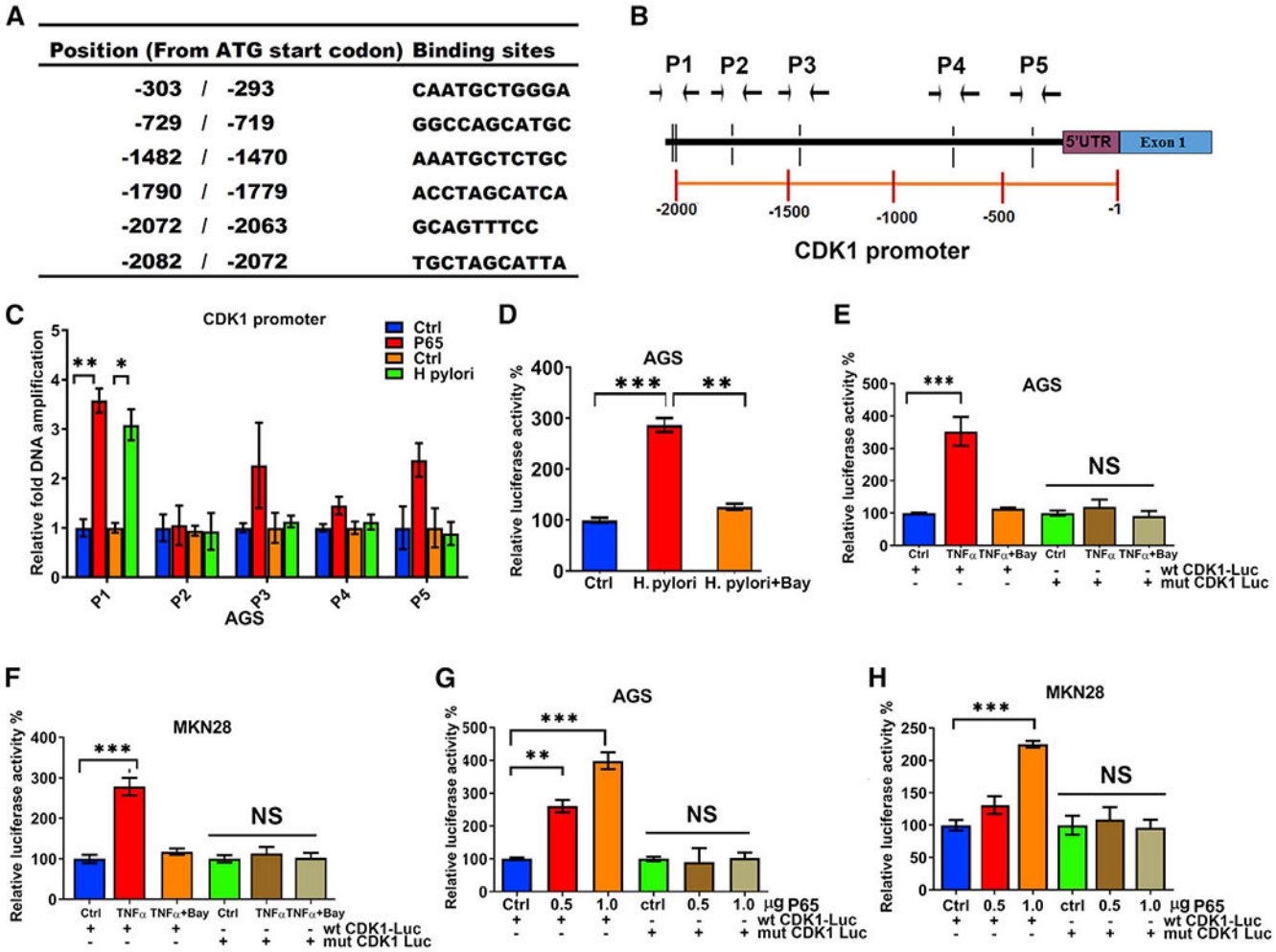

Figure 3. NF-κB transcriptionally upregulates CDK1 expression

(A and B) A table and a scheme showing putative NF-κB transcription factor binding sites on the CDK1 promoter and the CHIP primers designed in the CDK1 promoter (P1–P5).

(C) Chromatin immunoprecipitation (ChIP) assay using a specific antibody against P65 to immunoprecipitate formaldehyde-fixed chromatin in AGS cells, followed by quantitative real-time PCR with primers designed for the NF-κB-P65 binding site of the CDK1 promoter region with *H. pylori* infection or P65 plasmid transfection.

(D) Luciferase reporter assay for CDK1-Luc in AGS cells infected with *H. pylori* alone or combined with Bay 11-7082 treatment.

(E and F) Luciferase reporter assay for CDK1-Luc or mutCDK1-Luc in AGS and MKN28 cells treated with TNF-α alone or in combination with Bay 11-7082.

(G and H) Luciferase reporter assay for CDK1-Luc or mutCDK1-Luc constructs in AGS and MKN28 cells expressing P65 or empty vector.

Experiments were performed in triplicates. *$p < 0.05$, **$p < 0.01$, and ***$p < 0.001$.

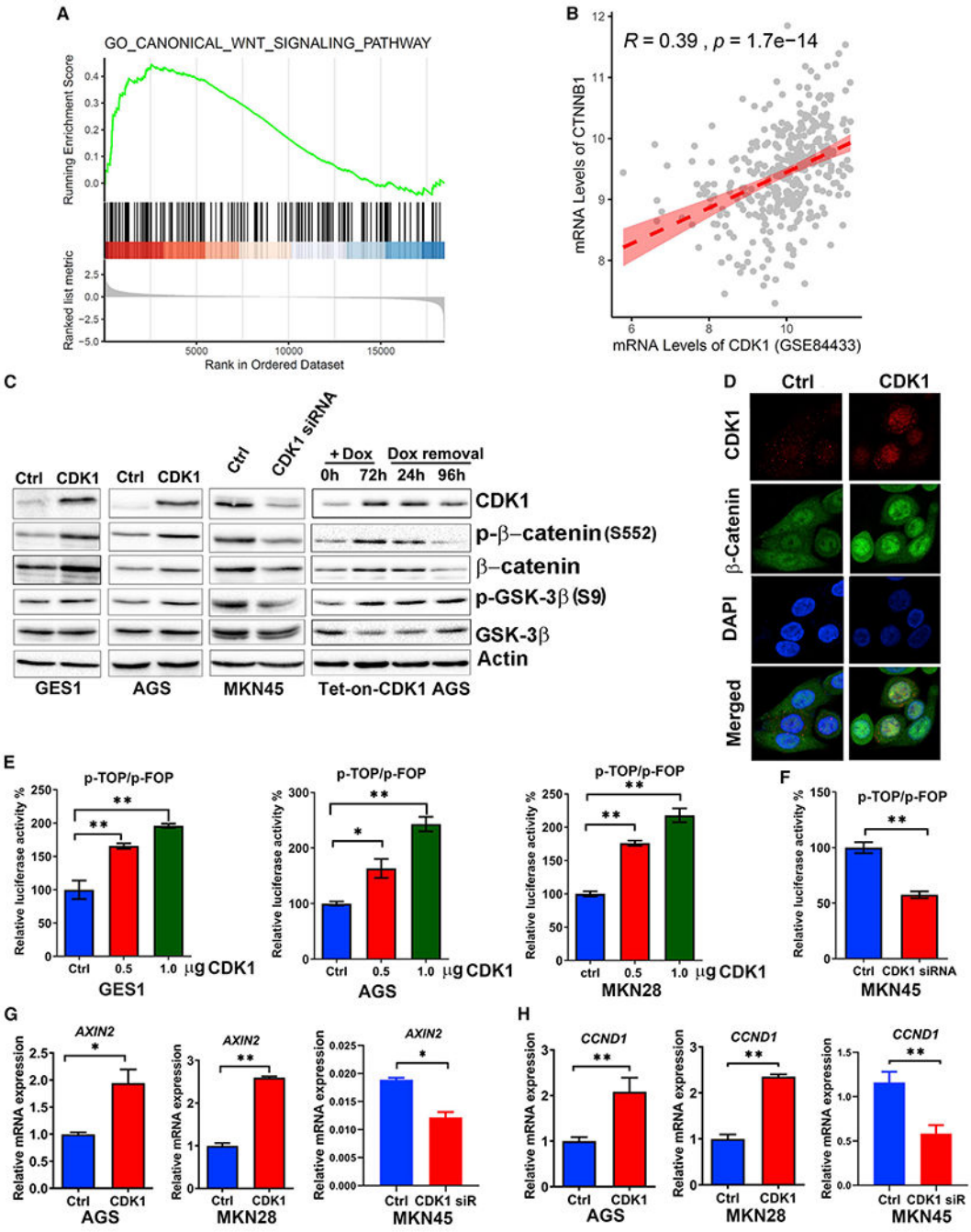

Figure 4. CDK1 regulates β-catenin protein levels and enhances β-catenin transcriptional activity

(A) Gene set enrichment analysis (GSEA) in a mouse model with *H. pylori* infection was performed by comparing infection cases with non-infection cases. Canonical Wnt signaling pathway was significantly enriched in *H. pylori* infection samples ($p < 0.01$).

(B) Pearson's correlation test revealed strong correlations between CDK1 expression and CTNNB1 level in the GEO: GSE84433 cohort ($R = 0.39$, $p < 0.01$).

(C) The immunoblot analyses were performed to determine β-catenin and p-GSK-3β (S9) expression in GES1 and AGS cells with overexpression of CDK1 or its knockdown by CDK1-specific siRNA in MKN45 cells.
(D) Representative immunofluorescent images of β-catenin (green) and CDK1 (red) in AGS cells' overexpression of CDK1; nuclei were stained with DAPI (blue).
(E and F) β-catenin luciferase reporter assays. TOP-flash contains wild-type TCF binding sites. FOP-flash, containing mutated TCF binding sites, is served as a negative control; *$p < 0.05$ and **$p < 0.01$.
(E) The gastric cancer (GC) cells were transfected with indicated amounts (0.5 or 1.0 μg) of CDK1 expression vector or empty vector control (Ctrl).
(F) The MKN45 cells were transfected with CDK1 siRNAs or scrambled siRNA (Ctrl).
(G and H) AGS or MKN28 cells were transfected with CDK1 expression plasmid or empty vector (Ctrl), and MKN45 cells were transfected with CDK1 siRNA or scramble siRNA control (Ctrl). Quantitative real-time PCR analysis of β-catenin targets, including AXIN2 and CCND1.
Experiments were performed in triplicates. *$p < 0.05$ and **$p < 0.01$.

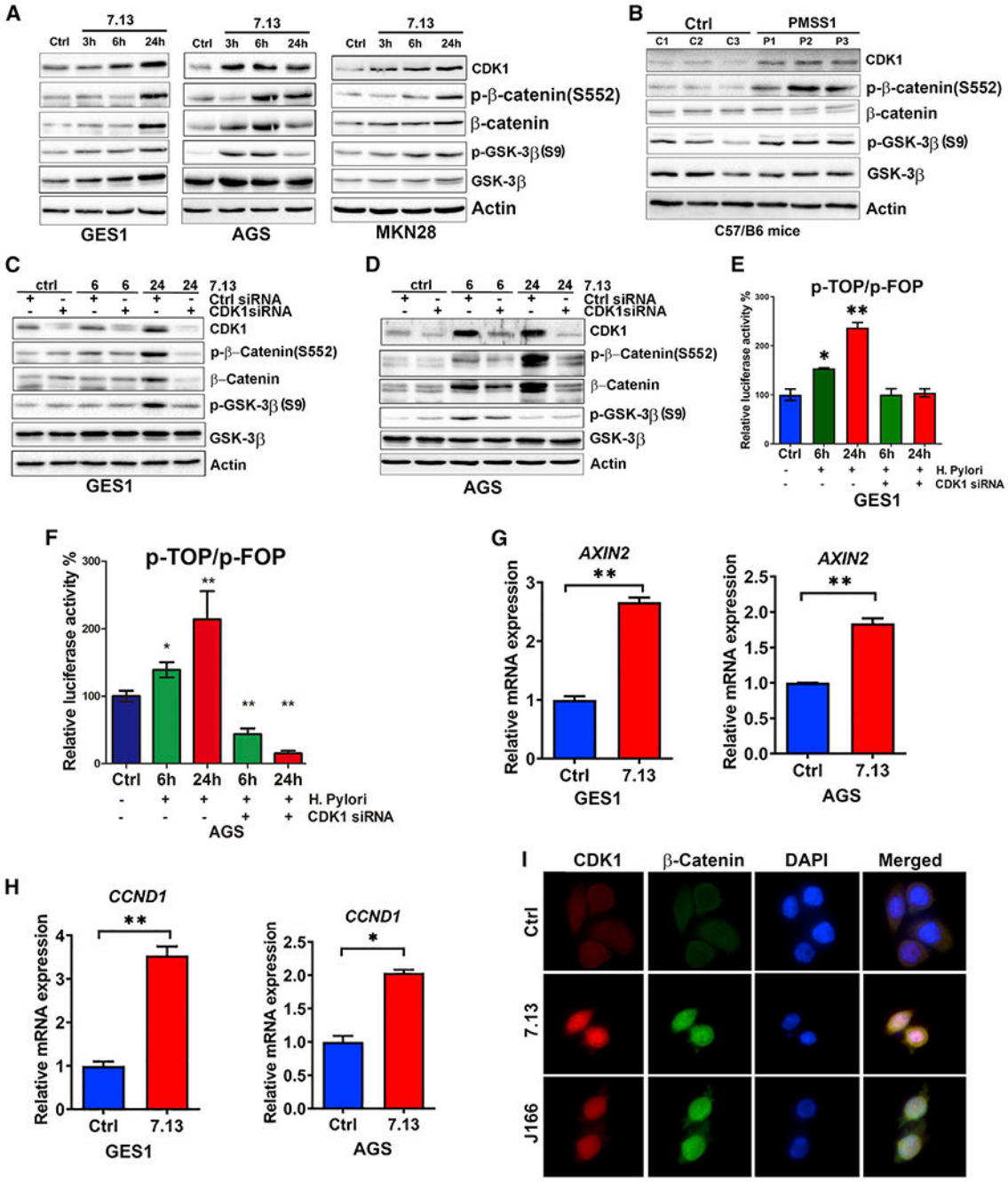

Figure 5. *H. pylori* infection increases β-catenin transcriptional activity through a CDK1-dependent manner

(A) Western blot analysis of p-β-catenin (S552), β-catenin, p-GSK-3β (S9), GSK-3β, and CDK1 in GES1, AGS, and MKN28 cells with *H. pylori* infection (7.13) at different time points (3, 6, and 24 h).

(B) The western blot analysis of p-β-catenin (S552), β-catenin, and CDK1 were performed in mice orogastrically challenged with Brucella broth or with PMSS1.

(C and D) Western blot analysis of p-β-catenin (S552), β-catenin, p-GSK-3β (S9), GSK-3β, and CDK1 with *H. pylori* infection and CDK1 siRNA knockdown in GES1 and AGS cells.

(E and F) Luciferase reporter assay for TOP or FOP in GES1 and AGS cells with *H. pylori* infection and CDK1 siRNA knockdown.
(G and H) Quantitative real-time PCR analysis of β-catenin targets, including AXIN2 and CCND1, were performed in GES1 or AGS cells with *H. pylori* infection (7.13).
(I) Representative immunofluorescent images of β-catenin (green) and CDK1 (red) in AGS cells with *H. pylori* infection; nuclei were stained with DAPI (blue).
Experiments were performed in triplicates. *$p < 0.05$ and **$p < 0.01$.

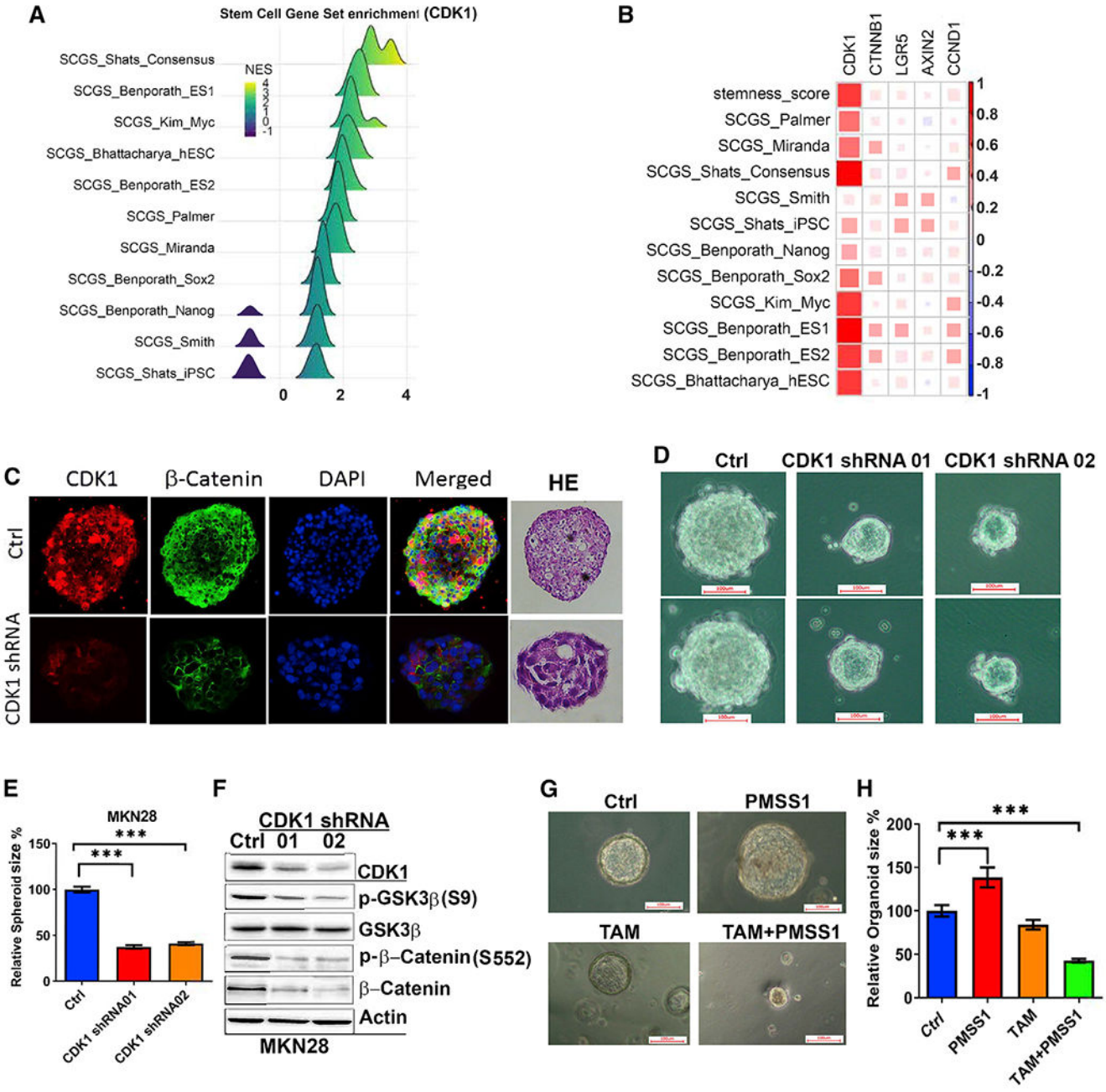

Figure 6. CDK1 depletion represses GC cell expansion

(A) GSEA in samples with high-CDK1 expression across the TCGA and GEO datasets.

(B) A weak to moderate correlation of the ssGSEA scores with β-catenin and its targets was observed.

(C) Representative immunofluorescent images of β-catenin (green) and CDK1 (red) in spheroids from MKN28 cells with stable knockdown CDK1; nuclei were stained with DAPI (blue).

(D) Spheroids (scale bars, 100 μm) derived from MKN28 cells with stable knockdown of CDK1 (CDK1 shRNA 01, CDK1 shRNA 02) displayed significantly smaller spheroids compared with the scrambled shRNA cells (Ctrl).

(E) The quantification of sphere size and the number was expressed as the mean ± SD of 3 independent fields: **$p < 0.01$ and ***$p < 0.001$.

(F) Western blot analysis of p-β-catenin (S552), β-catenin, p-GSK-3β (S9), GSK-3β, and CDK1 in spheroids derived from MKN28 cells with CDK1 shRNA knockdown.

(G and H) At the age of 8 weeks, $K19^{cre}CDK1^{fl/fl}$ (control) or $K19^{cre}CDK1^{fl/fl}$ mice received tamoxifen (50 mg/kg, intraperitoneally [i.p.]) for 10 days. At 10 weeks of age, the mice were infected with *H. pylori* (PMSS1 strain) for 1 month. The size of gastric organoids established from these mice was measured.

Experiments were performed in triplicate. **$p < 0.01$ and ***$p < 0.001$.

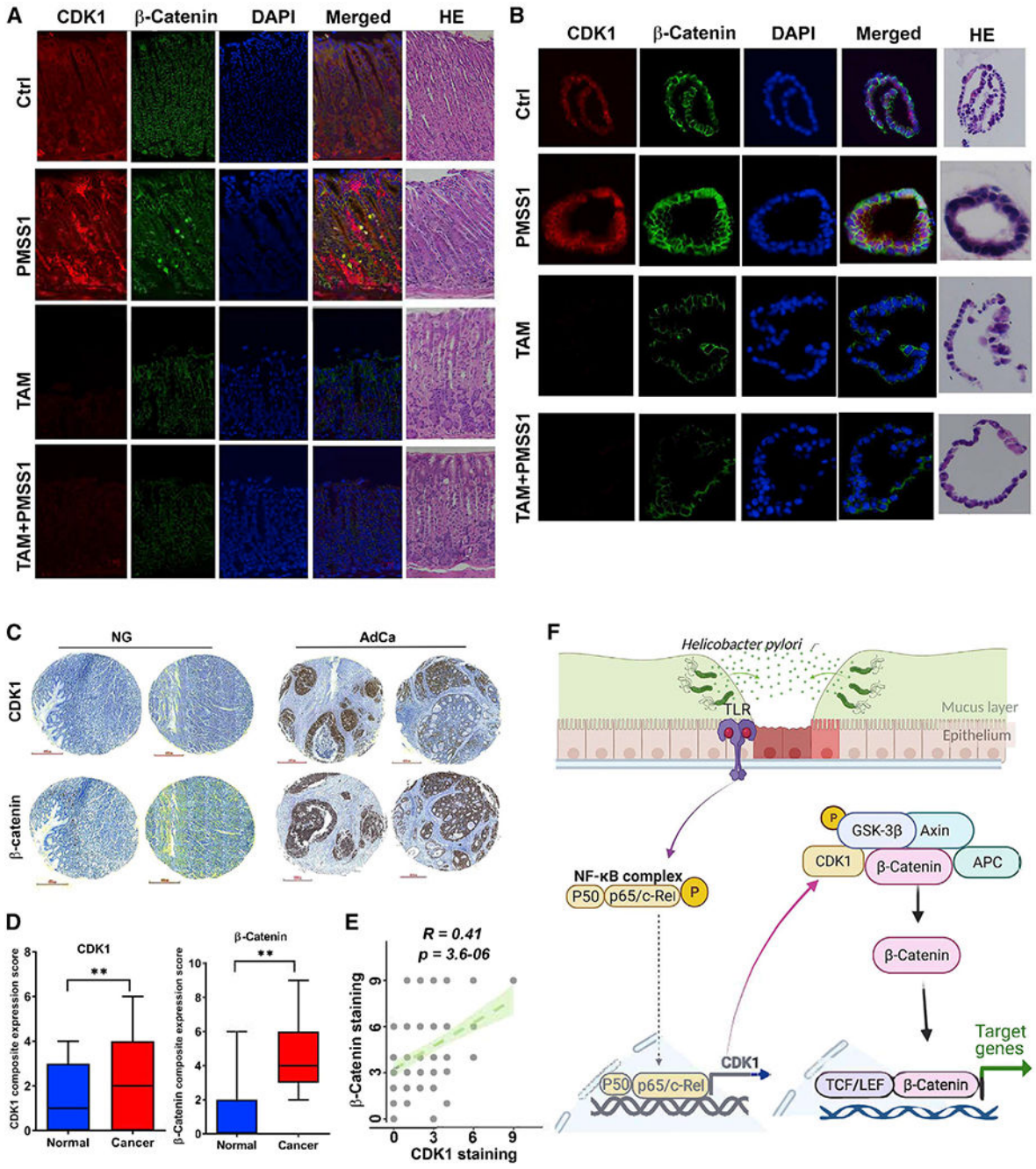

Figure 7. ***In vivo*** **studies of CDK1/β-catenin axis in gastric tumorigenesis**

(A) At the age of 8 weeks, $K19^{cre}CDK1^{fl/fl}$ (control) or $K19^{cre}CDK1^{fl/fl}$ mice received tamoxifen (50 mg/kg, i.p.) for 10 days. At 10 weeks of age, the mice were infected with *H. pylori* (PMSS1 strain) for 1 month. Immunofluorescence analyses of β-catenin (green) and CDK1 (red) from these mice were performed. H&E staining of representative histological features of gastric mucosa from mice.

(B) Immunofluorescence analyses of β-catenin (green) and CDK1 (red) were performed in gastric organoids established from $K19^{cre}CDK1^{fl/fl}$ (control) or $K19^{cre}CDK1^{fl/fl}$ mice

receiving tamoxifen treatment and/or *H. pylori* infection. Nuclei were stained with DAPI (blue). H&E staining of representative histological features of gastric organoids.

(C) Representative immunohistochemistry staining (scale bars, 100 μm) of CDK1 (n = 216) and β-catenin (n = 117) in human gastric tumors and adjacent non-tumor tissues.

(D) Composite expression score of CDK1 (n = 216) and β-catenin (n = 117) in tumor and non-tumor tissues.

(E) Spearman's correlation between IHC staining scores of CDK1 and β-catenin in tumor slides of 117 patients. TAM, tamoxifen.

(F) Illustration of the study model.

KEY RESOURCES TABLE

REAGENT or RESOURCE	SOURCE	IDENTIFIER
Antibodies		
Rabbit CDK1	Cell Signaling	Cat# 28439; RRID: AB_2798959
Mouse CDK1	Cell Signaling	Cat# 9116; RRID: AB_2074795
Rabbit CDK1	AbCam	Cat# ab133327; RRID: AB_11155333
p-GSK3β(S9)	Cell Signaling	Cat# 9323; RRID: AB_2115201
GSK3β	Cell Signaling	Cat# 5676; RRID: AB_10547140
GSK-3 α/β Antibody	R&D Systems	MAB26063
p-β-catenin(S552)	Cell Signaling	Cat# 5651; RRID: AB_10831053
p-β-catenin(S33/37/T41)	Cell Signaling	Cat# 9561; RRID: AB_331729
β-catenin	Cell Signaling	Cat# 8480; RRID: AB_11127855
p-NFKB(S536)	Cell Signaling	Cat# 3033; RRID: AB_331284
NFKB	Cell Signaling	Cat# 8242; RRID: AB_10859369
CagA	Austral Biologicals	HPP-5003-9
β-actin	Sigma-Aldrich	Cat# A1978; RRID: AB_476692
HRP-coupled anti-mouse, anti-rabbit	Promega	Cat# W4021; RRID:AB_430834Cat# W4011; RRID: AB_430833
CDC2/CDK1 Antibody	Novus	Cat# NBP1-85729; RRID: AB_11008973
MIST1/bHLHa15 (D7N4B) XP	Cell Signaling	Cat# 14896; RRID: AB_2798639
Normal IgG	EMD Millipore corp.	3281600
GSK3B Protein	Sino Biological	10044-H07B
CDK1 protein	RayBiotech Life	230-00782-50
Beta-catenin Protein	ABclonal	RP01241
Bacterial and virus strains		
J166, 7.13 and PMSS1 H. pylori strains, CagA + types	Gift from Dr. Peek (Vanderbilt University).	N/A
Biological samples		
Human gastric tissue samples	Fujian Medical University Union Hospital (FJMUUH, Fuzhou, China)	N/A
Chemicals, peptides, and recombinant proteins		
BAY 11-7082	Selleckchem	S2913
Human TNF-alpha	Peprotech	#300-01A-10ug
InSolution™ Cdk1 Inhibitor IV, RO-3306	Millipore Sigma	#217721-2MG
Dinaciclib	Cayman Chemical	# 14707
Tamoxifen	Millipore Sigma	T5648-1G
2nd Generation packaging	Abmgood	LV003
Polybrene	Sigma-aldrich	TR-1003
PolyJet Reagent	Signagen	#SL100688
B-27™ Supplement	Thermo fisher	#17504044

REAGENT or RESOURCE	SOURCE	IDENTIFIER
FGF-Basic (AA 1-155) Recombinant Human Protein	Thermofisher	PHG0264
EGF Recombinant Human Protein	Thermofisher	PHG0311
LipoJet Reagent	Signagen	#SL100468
Histo-gel	Richard-Allan, White Plains, NY	HG-4000-012
Critical commercial assays		
Duolink In Situ PLA Probe Anti-Rabbit PLUS	Sigma-aldrich	DUO92002
ChIP-IT Express Enzymatic	Active motif	#53039
ChIP-IT High Sensitivity	Active motif	#53040
Tru-seq RNA sample prep kit	illumina	RS-122-2001
Deposited data		
Raw and analyzed data	This paper	GEO DataSets: human gastric cancer datasets (GSE122401, GSE84433, GSE54129) and mouse datasets (GSE13873)
Gene Set Enrichment Analysis (GSEA) and Single-sample Gene Set Enrichment Analysis (ssGSEA) data	This paper	MSigDB (https://www.gsea-msigdb.org/gsea/index.jsp)
Experimental models: Cell lines		
MKN28	Riken Cell Bank (Tsukuba, Japan	N/A
MKN45	Riken Cell Bank (Tsukuba, Japan	N/A
AGS	American Type Culture Collection (ATCC, Manassas, VA)	N/A
GES1	Gift from Dr. Dawit Kidane-Mulat (The University of Texas-Austin, Austin, TX)	N/A
Experimental models: Organisms/strains		
129S(B6N)-*Cdk1*^{tm1Eddy}/J (*Cdk1*$^{flox/flox}$) mice and *Krt19*$^{Cre/ERT}$ mice	Jackson Laboratory (Bar Harbor, ME)	Strain #:028028 RRID: IMSR_JAX:028028
C57BL/6 mice	Charles River Laboratories (Wilmington, MA)	Strain Code: 027
pTetOne Vector	Takarbio	# 634303
Oligonucleotides		
CDK1 siRNA (NM_001786): GGUUAUAUCUCAUCUUUGATT	Thermo fisher	AM51331
pLV[shRNA]-Puro-U6>hCDK1[shRNA#1]: CAGGTTATATCTCATCTTTGA	vectorbuilder	VB201117-1178spk
pLV[shRNA]-Puro-U6>hCDK1[shRNA#2]: CCAGTTGACATTTGGAGTATA	vectorbuilder	VB201117-1180uan
pLV[shRNA]-Puro-U6>hCDK1[shRNA#4]: GCTGTACTTCGTCTTCTAATT	vectorbuilder	VB201228-1074bjm
pLV[shRNA]-Puro-U6>hCDK1[shRNA#3]: GATTTGGACAATCAGATTAAG	vectorbuilder	VB201228-1075auu
Primers for PCR and CHIP, see Table S5	This paper	N/A
Recombinant DNA		
Pcmv4 p65 Plasmid	Addgene	#21966
TOP flash (WT TCF Reporter Plasmid)	upstate biotechnology	#21-170
FOP flash (mutant TCF Reporter Plasmid)	upstate biotechnology	#21-169

REAGENT or RESOURCE	SOURCE	IDENTIFIER
pRP[Pro]-[CDK1]>Luciferase	vectorbuilder	VB201208-1092sem
Software and algorithms		
SPSS statistical package	SPSS, Chicago, IL, USA	NA
GraphPad Prism 8 software	GraphPad Software, Inc, San Diego, CA, USA	NA
JASPAR	https://jaspar.genereg.net/	NA